AD

USAAVLABS TECHNICAL REPORT 66-76

RESEARCH IN FABRICATION TECHNIQUES FOR FIBER GLASS REINFORCED PRIMARY AIRCRAFT STRUCTURES

By

Jay V. Daines

October 1966

U. S. ARMY AVIATION MATERIEL LABORATORIES
FORT EUSTIS, VIRGINIA

CONTRACT DA 44-177-AMC-326(T)

HITCO
GARDENA, CALIFORNIA

Disclaimers

The findings in this report are not to be construed as an official Department of the Army position unless so designated by other authorized documents.

When Government drawings, specifications, or other data are used for any purpose other than in connection with a definitely related Government procurement operation, the United States Government thereby incurs no responsibility nor any obligation whatsoever; and the fact that the Government may have formulated, furnished, or in any way supplied the said drawings, specifications, or other data is not to be regarded by implication or otherwise as in any manner licensing the holder or any other person or corporation, or conveying any rights or permission, to manufacture, use, or sell any patented invention that may in any way be related thereto.

Trade names cited in this report do not constitute an official endorsement or approval of the use of such commercial hardware or software.

Disposition Instructions

Destroy this report when no longer needed. Do not return it to originator.

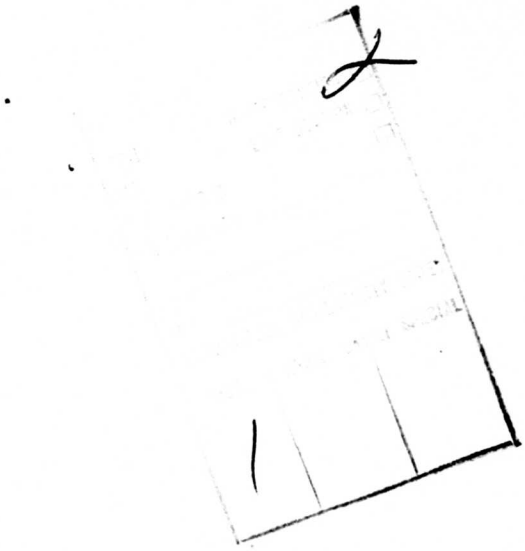

DEPARTMENT OF THE ARMY
U. S. ARMY AVIATION MATERIEL LABORATORIES
FORT EUSTIS, VIRGINIA 23604

This research effort was carried out under Contract DA 44-177-AMC-326(T) by HITCO.

This report has been reviewed by the U.S. Army Aviation Materiel Laboratories and is considered to be technically sound.

Task 1P121401A14176
Contract DA 44-177-AMC-326(T)
USAAVLABS Technical Report 66-76
October 1966

RESEARCH IN FABRICATION TECHNIQUES FOR FIBER GLASS REINFORCED PRIMARY AIRCRAFT STRUCTURES

by

Jay V. Daines

Prepared by

HITCO
Gardena, California

for

U. S. ARMY AVIATION MATERIEL LABORATORIES
FORT EUSTIS, VIRGINIA

SUMMARY

The primary purpose of this program was to demonstrate the feasibility of fabricating an irregular contoured box beam wing structural model from glass reinforced plastic (GRP).

This report covers the design, fabrication, and testing of GRP 1/2 scale models of a main torsion box assembly incorporating an NACA 64_2-215 airfoil. The structure was designed as a sandwich wall box beam, with non-woven oriented (NWO) GRP faces and a GRP honeycomb core.

Fabrication techniques for filament winding a double tapered box beam were investigated, and a technique was developed which made it possible to filament wind the 45-degree fibers as well as the hoop and axial oriented fibers. Six box beams were fabricated using both the hand lay-up process as a control and the developed filament winding process for fabricating the facings.

Unidirectional tape, 12 inches wide, made from E-HTS glass filaments and 20 end roving with both E-HTS and S-HTS glass filaments, preimpregnated with an epoxy resin system, were utilized in the fabrication of the facings.

Both primary (the resin system in the preimpregnated facing material) and secondary adhesive systems for bonding the honeycomb core to the faces were investigated on small flat panels to determine the best method to use in the fabrication of the box beams. The results of this study are shown in Tables II and IV.

Four of the models fabricated were cut into specimens and tested in flatwise tension, edgewise compression, and laminate tension. The results of these tests showed the beam with the filament wound faces to be 30 percent stronger in tension than the beam with the hand lay-up faces. The filament wound beam with the S-HTS glass filaments was 18 percent stronger than the filament wound beam with the E-HTS glass filaments.

The models fabricated using the filament winding process cost approximately 65 percent more than those fabricated using the hand lay-up technique. This is primarily due to the additional cure cycles required using the filament winding process (see Table III).

Both the hand lay-up and filament winding techniques of fabricating primary aircraft structures were found to be practical and within the current state of the art.

FOREWORD

This is the final report on HITCO S/O 121807 for the period 3 June 1965 to 5 July 1966 on U. S. Army Aviation Materiel Laboratories (USAAVLABS) Contract No. DA 44-177-AMC-326(T), Task 1P121401A14176. This report contains the design, fabrication procedures, test results, conclusions, and recommendations on the research conducted on fabrication techniques for fiber glass reinforced primary aircraft structures. Dr. Robert Echols, Chief, Physical Sciences Laboratory Division, and Mr. James P. Waller, Project Engineer, of USAAVLABS acted as technical monitors.

The program was conducted by the Advanced Design Engineering Group at HITCO, Gardena, California. The program was supervised by Mr. N. Myers and major responsibility for the program resided with Mr. J. Daines. Other significant contributors to the program include Messrs. D. Abildskov, G. Lee, R. Jackson, and S. Lee.

CONTENTS

ILLUSTRATIONS

TABLES

SYMBOLS

A area (inches^2)

a panel length (inches)

b panel width (inches)

C fiber spacing constant

c distance from C.G. (inches)

E modulus of elasticity (psi)

F allowable strength (psi)

G shear rigidity (psi)

I moment of inertia (inches^4)

K fiber straightness constant

L length (inches)

M moment (inch-pounds/inch)

m unit moment or load

N load (pounds/inch), number of layers

P reaction load (pounds/inch)

p pressure (psi)

Q moment area (inches^3/inch)

q shear load (pounds/inch)

R radius (inches)

T torsion (inch-pounds/inch)

t thickness (inches)

V shear force (pounds/inch)

W load (pounds/inch)

w load (pounds/inch)

$\bar{X}$ distance from C.G. to front spar (inches)

x distance in the x direction (inches)

y distance in the y direction (inches)

z distance in the z direction (inches)

α angle (degrees from y axis)

δ vertical deflection (inches)

θ rotation (radians)

σ stress (psi)

ϕ rotation (radians)

μ Poisson's ratio example μ_{yx} - relating strain in the x direction to strain in the y direction owing to stress in the y direction

SUBSCRIPTS

a at point a, air

b at point b, bending

c compression, core, at point c, chordwise

d at point d

e at point e

f facings

g fiber glass

L longitudinal direction

m due to moment

p due to reaction P

r resin

s shear

t tension

T transverse direction

v vertical direction

x x direction

y	y direction
z	z direction
all	allowable
cr	critical
xx	around the xx axis
zz	around the zz axis
α	at angle α
θ	due to rotation

INTRODUCTION

The demand for higher strength, lower cost, and lighter weight structural materials for primary aircraft structures has motivated this investigation of the main load-carrying structure of a light aircraft wing, using nonwoven oriented (NWO) fiber glass reinforced plastic.

The use of glass reinforced plastic (GRP) is not new in aircraft structures, with its usage dating back more than 10 years. However, the previous and current usage has been mainly limited to secondary load-carrying structural components and to glass cloth laminates. Although these laminates have performed very satisfactorily and are now extensively used throughout the aircraft, they do not represent the state of the art in current GRP technology. This technology has been recently developed (during the last 5 years) mainly under missile rocket motor cases and deep-diving submersible (hydrospace) research contracts. These programs have led to widespread acceptance of filament wound GRP as the primary load-carrying material.

These advancements in fabrication technology indicate that aircraft primary structural components can be fabricated from nonwoven oriented GRP at a savings of weight and possibly at reduced cost.

The purpose of this program was to design and fabricate six subscale light aircraft sections (sandwich wall box beams) using nonwoven oriented glass fiber faces and GRP honeycomb core. The airfoil configuration selected was an NACA 64_2-215 with the spars at 35 percent and 75 percent chord. The design loading conditions are shown in Appendix I. Four of the beams were cut into test specimens to evaluate the mechanical properties of the facing material and bond strength to the core. The remaining two beams are retained for future testing as a complete beam.

The main body of this report is primarily concerned with reporting design, fabrication techniques, and test results. Drawings, fabrication procedures, and structural analysis are presented in Appendices I through IV.

DISCUSSION OF RESULTS

DESIGN OF BOX BEAM

The primary load-carrying structure of a light pleasure aircraft wing with an NACA 64_2-215 airfoil configuration was analyzed and designed. The wing was 180 inches long from root chord to tip chord. The chord length at station 0 (root chord) was 72.00 inches and at station 180 (tip chord) was 48.00 inches (see Figure 24). The CAR-3 airload criterion was applied to determine the critical flight structural loading as shown in Appendix I. The wing was designed for the structural load to be carried between 35 percent and 75 percent of the chord. This results in a chord length between front and rear spars of 28.00 inches at root chord and 19.20 inches at tip chord. The cross section of an NACA 64_2-215 airfoil is slightly unsymmetrical; however, it was assumed to be symmetrical in the calculations of the section properties, since the error was very slight (approximately 1 percent).

The fiber orientations considered in the design optimization are shown below.

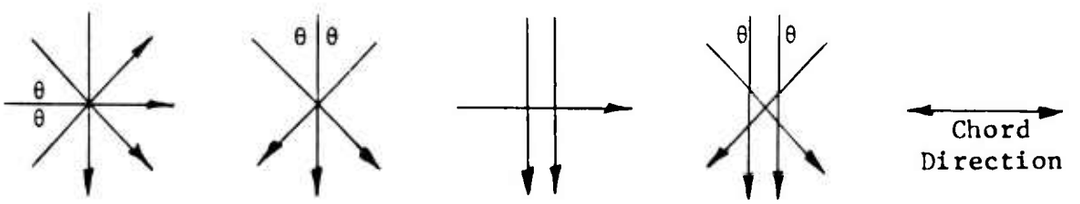

Config. 1 Config. 2 Config. 3 Config. 4

E-HTS and S-HTS 20 end glass rovings were preimpregnated with an E787 resin system for the filament wound beams. This material has a standard thickness of 0.010 to 0.011 inch. The unidirectional tape was preimpregnated with an XP-251 resin system. The thickness of this material can be varied depending on the resin content and the end count. The standard end count was 200 ends per inch, which resulted in a slightly thinner ply thickness than the 20 end rovings.

A facing thickness of 0.030 to 0.040 inch was required for stress consideration, depending on the fiber orientation; therefore, a three- or four-ply facing is required.

Configuration 1 with θ equal to 45 degrees was chosen for the following reasons: (1) the 45-degree fibers supply shear strength and rigidity to the structure, (2) the chordwise fiber gives the necessary bending stiffness to control the chordwise deflection, and (3) the spanwise fiber is required for axial stress and buckling considerations. The mechanical properties for this configuration were theoretically determined as shown in Appendix I.

HRP 3/16-GF 11-4.0 honeycomb (GRP) was used as the core material. The core

thickness required to stabilize the faces against buckling was calculated with the above facing thickness and fiber orientations. Complete analyses of buckling, stress, and deflection are shown in Appendices I and II, and a stress and deflection analysis summary is shown in Table XVIII.

DESIGN OF SCALE MODEL

The primary load-carrying structure of a wing section 1[illegible] inches long with a root chord of 28.80 inches between spars and a tip chord of 19.20 inches between spars was scaled down for a subscale fabrication model. The external dimensions (NACA 64_2-215 airfoil configuration) were scaled down to 1/2 scale of the inboard 1/2 section of the wing. The facing thickness was not scaled, since the ply thickness is standard (as explained above) and to special order a custom-made roving was beyond the scope of this program. The core thickness was scaled such that the model would buckle at the same axial load, in pounds per inch, as the full-scale wing section. This gives a core scale factor of approximately 1/2. The dimensions of the scale model after trim are as shown below and on drawing SKRD 0607, Appendix IV:

Spanwise length = 45.0 inches
Chordwise width at station 0 = 14.4 inches
Chordwise width at station 90 (tip of model) = 12.0 inches
Core thickness = 0.460 inch
Facing thickness = 0.040 inch
Front spar height at root = 5.399 inches
Front spar height at tip = 4.491 inches
Rear spar height at root = 2.374 inches
Rear spar height at tip = 1.976 inches

FILAMENT WINDING TECHNIQUES

Filament winding techniques were developed for winding the hoops, 45-degree fibers, and longitudinals. A temporary wood mandrel was fabricated to investigate methods that could be used in filament winding a double tapered box beam section. There was no problem in winding the hoops (chordwise filaments) the same as hoop winding a cylinder. The longitudinal (spanwise) fibers were hoop wound by rotating the mandrel end over end. Side plates were required on the mandrel to give a constant width for winding the longitudinal fibers. Figure 2 shows the side plates and mandrel for winding the longitudinal fibers. Winding the 45-degree fibers posed a greater problem because of the taper in both directions along the length of the mandrel. Two general methods were investigated for filament winding the 45-degree fibers; the helical winding approach and the hoop winding approach. These methods, with the problems and advantages of each, are outlined below.

Helical Winding

The initial attempt to filament wind the box beam was to use the helical winding method which has been used for years primarily on cylinders and end domes. Limited helical winding has been accomplished for cone shaped pressure vessels. The winding angle varies along the cone section because of circumferential change. The tapered box beam is some-

what similar to a cone; therefore, side plates were placed on the wood mandrel to give a constant circumference.

The first problems encountered in attempting to wind the beam helically were the change of winding angle along each surface and fiber slippage around the corners. The distance the let-off carriage travels from the time the fiber comes in contact with one corner until it comes in contact with the next corner divided by the width of the face between these two corners must always be a constant for all surfaces for the winding angle to be constant. This can be accomplished if the let-off eye is the same distance from all corners as the mandrel rotates. Since the mandrel is tapered in both directions, the let-off eye distance will vary from one end to the other end of the mandrel. By holding the let-off eye as close to the corner as possible, the angle variation was not too excessive, approximately 4 degrees. Another solution would be to have an in-and-out control on the let-off eye to hold it in the same relative position to the mandrel. The slippage along the edge could be controlled with double-back tape or a system of extruded pins or nails to catch the fibers on the corners.

The major problem in attempting to wind the box beam helically was experienced in winding over the trapezoidal ends. The dwell time of the let-off eye past the end of a cylinder is constant for every circuit; however, on the box beam the effective dwell time varies for each circuit. The effective dwell time is an inverse function of the distance between the let-off eye and the mandrel end at the point of fiber contact. This distance varies by approximately one-half the mandrel width (chord dimension) for one complete layer, which causes considerable fiber gapping on one edge of the mandrel and fiber overlapping on the other edge. The only way to control this effect completely is to have the let-off eye back-and-forth motion completely separate from the mandrel rotation control. One of the controls would then need to be hand operated, since the stall time would be different for every circuit. A method of stabilizing the fiber on the ends is also required.

This approach to filament winding a box beam did not appear practical, if at all possible, because of the problems stated above; therefore, an alternate approach of hoop winding the 45-degree fibers was investigated.

Hoop Winding

The alternate method of filament winding the 45-degree fibers was to hoop wind them. This was accomplished by making extension arms to the mandrel so as to place it in the winding machine with the axis oriented at 45 degrees to the winding machine axis. The mandrel is then rotated, and the fibers are hoop wound on the mandrel as shown in Figure 1. The arms are reversed for the second layer of 45-degree fibers. The fibers were held from sliding along the edges with threaded rods which were tied into the mandrel. Other methods may be used such as nails or a grooved plate; however, the threaded rods worked

very well and were inexpensive. The following fabrication modifications and mandrel design changes were required for hoop winding the 45-degree fibers.

1. Threaded rods were designed with the thread dimension equal to the roving width so that each roving would fit into a separate groove. This kept the rovings from gapping and overlapping and provided an even ply thickness.

2. Filament winding the faces required three more cure cycles than the hand lay-up process. The inside spar faces must be precured, since no pressure can be applied to them with the attachments for winding the inside face. The inside face must be cured and trimmed before the honeycomb core and outside spar faces can be laid up. The honeycomb must be cured to the inside flange face and to the inside and outside spar faces (see Figure 8), since pressure cannot be applied to the spar area with the attachments for winding the outside flange face.

3. The mandrel length had to be increased considerably because of the trim length required by winding the 45-degree fiber by this method. This trim length is equal to the part width at each end; however, the threaded rods were run around the ends, which shortened the trim length to 10 inches on each end.

4. End fixtures for rotating the mandrel at 45 degrees, side plates, and end attachments for the threaded rods were required in the mandrel design.

Figures 3, 4, 5, and 6 show the attachments and the winding technique for winding the longitudinals, 45-degree fibers, and hoops, respectively. The sequential order of winding the four layers must be the same for the inside and outside faces, longitudinals, 45-degree layers, and then hoops. The longitudinals cannot be wound over the attachments for the 45-degree fibers and, therefore, must be wound first.

MANDREL DESIGN

The loads applied to the box beam mandrel during the winding of the faces are generally insignificant. Winding loads caused by the hoops and longitudinals with only one layer of 20 end roving can be neglected. The 45-degree fibers, however, cause shear stresses in the mandrel which must be carried with very little mandrel shear deflection, since a slight amount of deflection will cause the 45-degree fibers to lose tension. The primary loads on the mandrel are from autoclave pressure while curing the box beams.

The mandrel was designed with longitudinal plates at the front and rear spar locations. These longitudinal plates were riveted to end plates and intermediate ribs which were precontoured to the NACA 64_2-215 airfoil configuration. Thin aluminum sheets were then formed over the ribs and welded to the longitudinal plates. This method of mandrel fabrication was consider-

ably less expensive than machining thick aluminum skins to the desired contour. The mandrel was designed for both internal and external pressure, since the thin skin would not carry the autoclave pressure during cure of the parts. The mandrel also had to be leakproof with this design; otherwise, pressure would leak between the mandrel and bag and no effective pressure would be applied against the part being cured.

The mandrel was also designed with the capability of attaching the side plates for winding the longitudinals (see Figure 2) and attaching the threaded rods, rod ties, and rotating arms for winding the 45-degree fibers (see Figures 4 and 5).

The threaded rods were designed such that each thread held one 20 end roving which prevented gapping and overlapping of the fibers. A separate set of rods was required for each layer of 45-degree fibers. Figures 3 through 6 show the winding attachments during winding the longitudinals, 45-degree fibers, and hoops, respectively.

The mandrel began to leak as the inside face of box beam No. 2 was placed in the autoclave to cure. Several attempts were made to seal the mandrel:

1. The inside of the mandrel was coated with resin which temporarily sealed the corners. As another face was wound and cured, the resin cracked from the shear loads in the mandrel during winding and the differences in the coefficients of thermal expansion between the resin and the aluminum during cure. This caused the mandrel to begin leaking again.

2. Sealing of the mandrel was again attempted by externally rewelding all the seams. The surface of the mandrel was hard anodized and, therefore, had to be sanded along the seams before welding. In attempting to weld the seams, the thin skins began to warp and separate from the side plates. The mandrel was cleaned and repaired in the warped areas.

3. Teflon adhesive tape was bonded along the edges (spar sections) and on the ends of the mandrel. The tape on the ends soon began to leak because the end fixtures' constantly being put on and taken off tore up the Teflon.

4. A flexible plastisol molding compound was poured into the mandrel and sloshed around to seal the end sections; however, the plastisol apparently did not fill all the cracks in the resin and the mandrel still leaked at the ends.

Further attempts to seal the mandrel were considered unjustified, and the remainder of the beams were cured under vacuum.

FABRICATION

A box beam fabrication summary is presented in Table I. This table covers the method of fabrication, materials used, the method of cure for each box

beam, and box beam weight. The step-by-step fabrication procedures are provided in Appendix III, and a photo representation of the fabrication procedures for the filament wound beams is shown in Figures 3 through 10. Figure 3 shows the winding of the longitudinal fibers by rotating the mandrel end over end. Figures 4 and 5 illustrate the winding of the 45-degree fibers. The threaded rods along the edges prevent the fiber from sliding as they are hoop wound on the mandrel, which is set in the machine at 45 degrees. Figure 6 shows the winding of the hoop fibers. The inside face must be cured after the winding of the hoop fibers, since the spar honeycomb and outside face cannot be assembled with the hoop and 45-degree windings restricting access to the edges. After curing and trimming the inside face, the honeycomb and syntactic foam corner sections are laid inside the outside spar face as shown in Figure 7. These assembled spars are then placed over the inside face, and the honeycomb is placed over the flanges as shown in Figure 8. The beam is then bagged and cured to bond the honeycomb to the spar faces and the inside flange face. The outside flange facing is then wound the same as the inside facing shown in Figures 3 through 6.

The procedures for fabricating the hand lay-up beam are basically the same as those for the filament wound beams described above, except that the beam was laid up in one stage by eliminating the three cure cycles required on the filament wound beam.

Figures 9 and 10 show a completed beam after it has been removed from the mandrel and trimmed.

Two methods were investigated for bonding the honeycomb core to the faces. These were the use of a secondary adhesive film and the use of resin from the preimpregnated facing material. Box beam No. 1 was hand laid up by using Metlbond 500 adhesive film as a secondary adhesive. The flatwise tensile strength of this beam was very low (only 448 psi average); therefore, panels 8 inches square were fabricated and tested using various secondary adhesive systems and also some primary resin systems for bonding the honeycomb core to the faces. The results of this study are shown in Table II. The resin system used on the 20 end roving (E787) only gave 344 psi in tensile strength or 35 percent to 40 percent as high as the panels with the secondary adhesive bonds. The Metlbond 500, which is a resin adhesive system, gave the highest result of 963 psi. The Metlbond 329 and the AF-110A adhesive systems gave strength values of 899 psi and 808 psi, respectively; these values were 8 percent and 19 percent lower than the Metlbond 500 resin system values.

Metlbond 329 adhesive was used on box beams No. 2 through 6 because of its high strength characteristics and ready availability. Thin aluminum caul sheets, 0.016 inch thick, were placed over the beams. These caul sheets were designed thin enough to conform to the contour of the mandrel and stiff enough to avoid local wrinkling. The purpose of the caul sheets was to provide a smooth exterior surface on the box beams. The results of the first beams were so good, a finish of 20 to 45 on beam No. 1 and approximately 150 on beam No. 2, that no other method was investigated. Resin was added on beams No. 5 and 6 between the 45-degree fibers and the hoop fibers to give more resin flow and, therefore, to help fill the voids next to the surface

and to give a smoother finish.

A tear ply was placed on the outside of the inside face prior to bagging and curing. This ply is torn off after cure and leaves a rough surface for bonding the honeycomb core to the inside skin. The tear ply consists of one ply of 120 cloth preimpregnated with E787 resin. This ply forms a relatively low bond strength to the NWO fibers and, therefore, can be easily ripped off after cure. The tear ply eliminates sanding the faces, which could cut some of the fibers.

The design of the spar to flange joint is shown on drawing SKRD 0607, Appendix IV. The syntactic foam (42 pounds per cubic foot density) was cast in a flat mold and machined to the required dimensions. The foam was then bonded together with Eastman's 910 adhesive prior to being placed in the outside spar face as shown in Figure 7.

EVALUATION OF TEST RESULTS

Preproduction Fabrication and Setup Time

The setup and fabrication time is shown in Table III.

The total time required for a filament wound beam is 165 hours, compared to 102 hours for a hand lay-up beam. The fabrication time for a filament wound beam is 110 hours (excluding items 2 and 3 in Table III), compared to 94 hours for the hand lay-up beam. The increased time for the filament wound beam is caused by the three extra cure cycles which add 26 hours. Five hours are saved for each face in filament winding versus the hand lay-up process; however, this is a small portion of the total hours required. The labor cost is 62 percent higher on the filament wound preproduction model.

Surface Smoothness

The surface smoothness of the completed beam was mainly a function of the caul sheet, fiber evenness, resin content of the surface layer, and cure pressure. The caul sheet bridges along the peaks caused by fiber unevenness and forces these high points down as the resin begins to flow. Enough resin is required in the surface layer to fill all the voids between the glass and the caul sheet. A high cure pressure helps to force the resin into the voids and gaps and, therefore, gives a smoother finish.

Box beam No. 1 had a finish of 20 to 45 per MIL-STD-10, and beams No. 2 through 6 had a finish of approximately 150. The fibers were much more consistent in the unidirection tape, and box beam No. 1 was cured at a much higher pressure (see Table I) than the remainder of the beams; these facts account for the much smoother surface. Resin was added between the last two layers on box beams No. 5 and 6 to help fill the voids and give better flow, since the material was becoming slightly dry on these beams.

Test Results

Box beams No. 1 through 4 were cut into test specimens for flatwise tensile, edgewise compression, and laminate tensile tests. The flatwise tensile and edgewise compression specimens were tested per MIL-STD-401A, and the laminate tensile specimens were tested per FTMB 406, Method 1011, Type I. Tables IV through XV show the test results of box beams No. 1 through 4, and a summary of the test results is shown in Table XVI.

Box beam No. 1 was hand laid up with E-HTS/XP251 facing material and Metlbond 400 adhesive film for bonding the honeycomb core to the faces. The adhesive film was dry and did not appear to flow when heated, which could account for the very low flatwise tensile strength of 448 psi shown in Table IV. Because of the low results on the first beam, 8-inch-square flat panels were fabricated with different adhesive systems to determine a suitable system for the remainder of the box beams. These panels were cut and tested in flatwise tension. The results are shown in Table II and explained on page 7 under fabrication. The edgewise compression test results on box beam No. 1 were lower than expected; 35,680 psi compared to a theoretical strength of 49,000 psi, or 37 percent lower then the theoretical strength. The laminate tensile test results were slightly higher than those predicted; 46,232 psi compared to a theoretical strength of 45,000 psi, or 3 percent higher than the theoretical. The impregnated material used on this beam had been refrigerated for several months due to the delay in receiving the mandrel and, therefore, had lost its tackiness and become quite dry before box beam No. 1 was fabricated. The beam had visible dry streaks after cure. This could partially account for the low strength in the edgewise compression and laminate tensile tests.

Box beams No. 2 and 3 were filament wound with E-HTS/E787 20 end roving. These beams were fabricated in the same manner as beam No. 1 except that a tear ply of 120 cloth preimpregnated with E787 was placed next to the hoop layer on the inside skin prior to bagging and cure and the hoops were discontinued on beam No. 3 at the midspan to give a tailoring effect. The flatwise tensile strength of box beam No. 3 was 26 percent lower than on box beam No. 2. Box beam No. 3 appeared to lose vacuum pressure during cure, which would account for the lower values. Box beam No. 3 also had streaks in the faces which could have been caused by the loss of vacuum and, consequently, the lack of proper flow during cure. The edgewise compression and laminate tensile test results were in good agreement between the two beams, with the edgewise compression strength being approximately 4 percent below the theoretical values and the laminate tensile strength being 34 percent above the theoretical values.

Box beam No. 3 was filament wound with the hoop layer (chordwise layer) terminating at midspan to give a tailoring effect. Specimens from both the three-ply area with no hoops and the four-ply area with hoops were cut and tested. The average failure load in the three-ply area was 16 percent lower than in the four-ply area on the edgewise compression

tests; however, this gives a stress of 11 percent higher for the three-ply area because of the thickness difference of 25 percent. The laminate tensile tests were 25 percent lower in the four-ply area in strength, and the tensile failure load averaged 7 percent higher in the four-ply area.

Box beam No. 4 was filament wound identically to box beam No. 3 except that S-HTS/E787 material was used in the faces. The flatwise tensile strength was 932 psi, compared to 971 psi on box beam No. 2. The laminate tensile strength increased 18 percent and 30 percent, respectively, in the four-ply and three-ply areas by using the S-HTS glass faces instead of the E-HTS glass faces.

The compressive strengths on box beam No. 4 were very close to those on beams No. 2 and 3 (see Table XVI).

The edgewise compression specimens were strain gaged with a longitudinal gage on each side and a hoop gage on one side. The ends of the specimens were potted with Epon 934 adhesive to prevent premature edge failures. Figures 11 through 14 show typical failure modes. These specimens were sized and tested per MIL-STD-401A; however, somewhat higher results should be obtainable from other specimen configurations where the 45-degree fibers are not cut.

The minimum recommended cure pressure for the Metlbond 329 adhesive film is 15 psi. Box beams No. 2 through 6 were cured at a pressure of 5 to 10 psi; therefore, the flatwise tensile strength may be increased above the values shown in Table XVI by curing in an autoclave at 15 to 50 psi, as was originally anticipated.

The laminate tensile test results obtained from box beams No. 1 through 4 showed an increase of 30 percent in the strength of a filament wound beam over a hand laid up beam. The use of S-HTS glass increased the tensile strength 18 percent over the beams with E-HTS glass fibers. Figures 15 and 16 show typical failure modes.

The compressive moduli of elasticity on beams No. 1, 2, and 3 were 3.88, 3.42, and 3.36 million psi, compared to a theoretical modulus of elasticity of 3.375×10^6 psi. This is an increase from 0.5 percent to 15 percent in measured values over the theoretical value. The primary moduli of elasticity (see Figure 18) obtained from the tensile specimens were 2.91, 3.08, and 3.12×10^6 psi, or from 8 percent to 16 percent below the theoretical values. The secondary tensile moduli of elasticity were 1.65, 1.79, and 1.78×10^6 psi on beams No. 1, 2, and 3, respectively, which is approximately 58 percent of the primary modulus of elasticity. The modulus of elasticity of the S-HTS glass beam increased approximately 5 percent and 9 percent in compression and tension, respectively, over the E-HTS glass beams. The compressive modulus of elasticity increased from 3 percent to 6 percent in the three-ply area over the four-ply area of beams No. 3 and 4, and the primary tensile modulus of elasticity increased from 16 percent to 22 percent. The tensile load-strain curves are approximately parallel in the three-

ply and four-ply areas; this indicates that the modulus and strength of the hoop fibers is very low in the transverse direction. The modulus and strength is, therefore, mainly a function of total facing thickness which gives the 25 percent difference in tensile strength and tensile primary modulus in the three- and four-ply areas. Typical stress-strain curves are shown in Figures 17 and 18.

The theoretical Poisson's ratios were much lower, being about 37 percent of the values obtained from the test results. This is mainly due to fiber reorientation. In compression, the 45-degree fibers tend to rotate perpendicular to the direction of the load; however, they are partially restrained by the resin binder, friction between the filaments, and the restraint of the hoop and axial fibers. The Poisson's ratios in the three-ply area were 41 percent and 45 percent higher than those in the four-ply area of beams No. 3 and 4, respectively. This increase is mainly due to the elimination of the hoop fibers which helped stabilize the 45-degree fibers and kept them from rotating as much and the relationship of the stiffness ratio in the longitudinal and hoop direction with and without the hoop fibers.

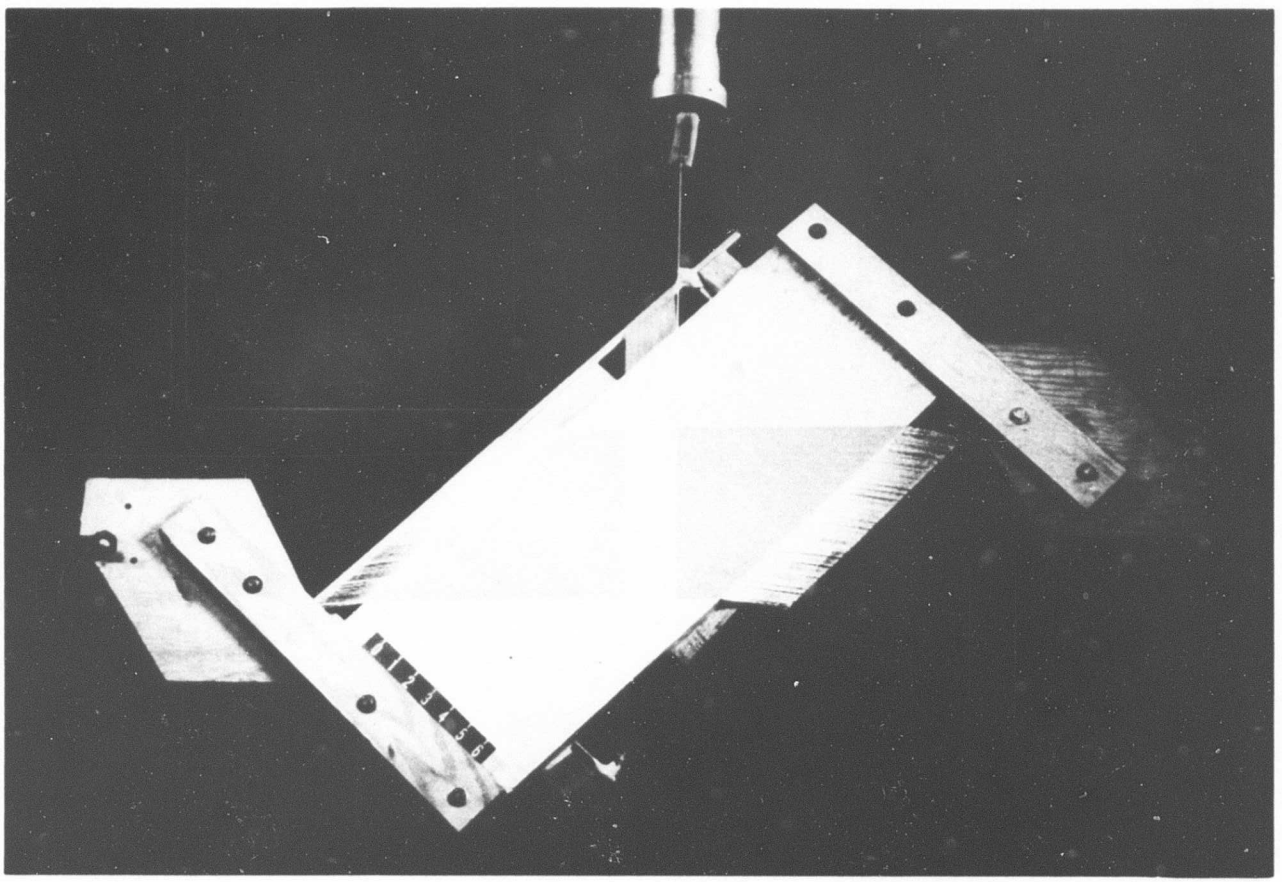

Figure 1. Preliminary Winding on Wood Mandrel.

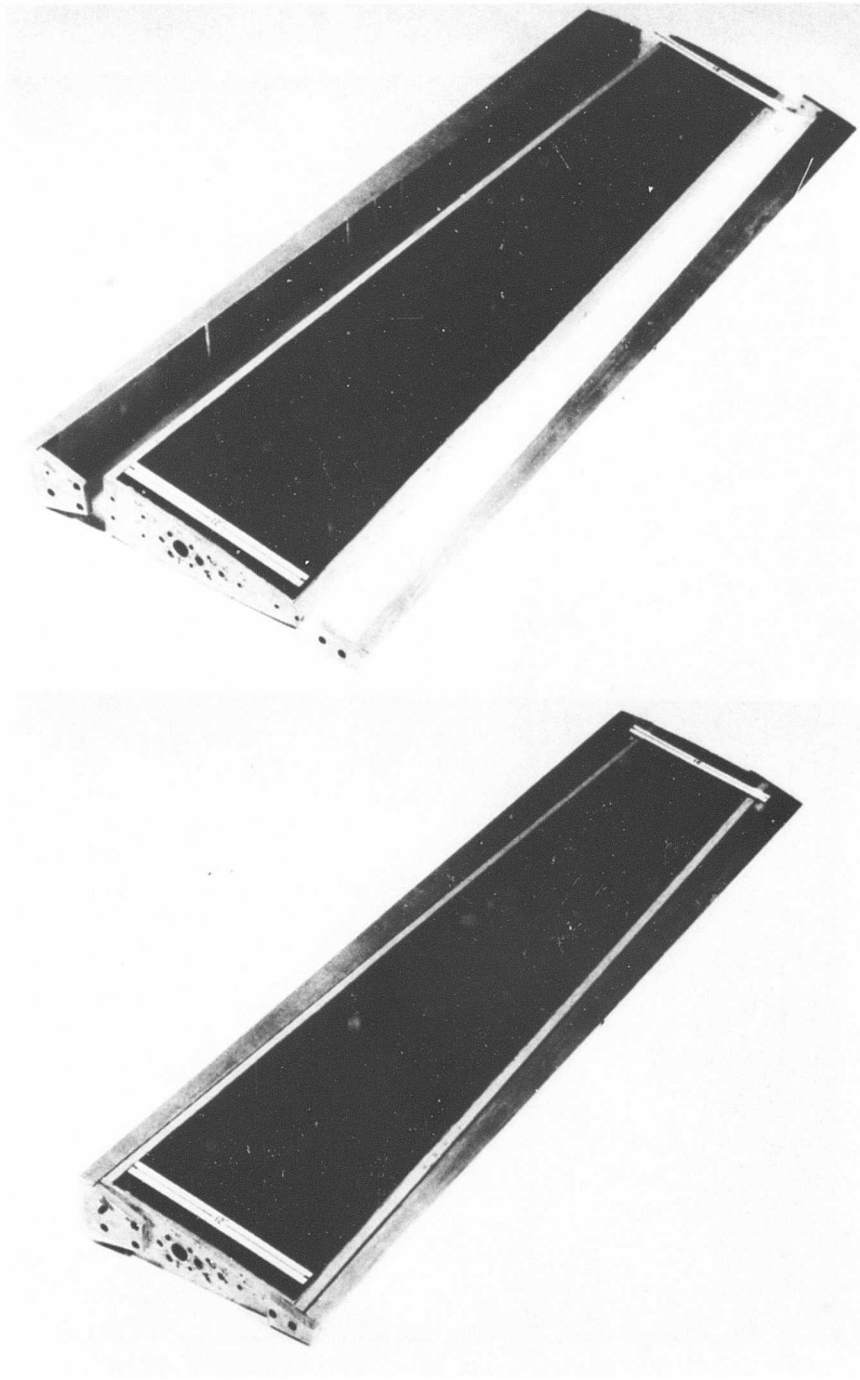

Figure 2. Mandrel Before and After Side Fixture Assembly.

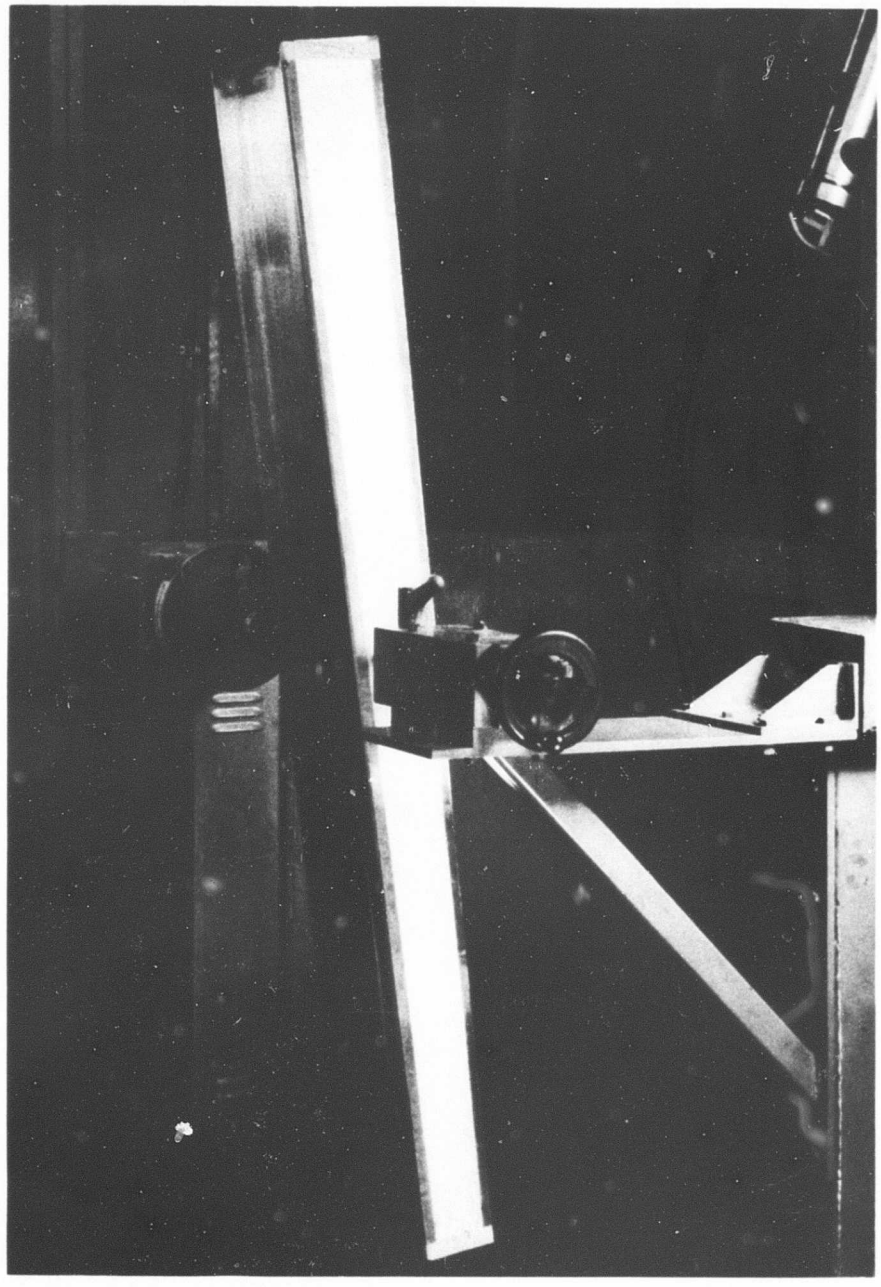

Figure 3. Winding Longitudinal Fibers.

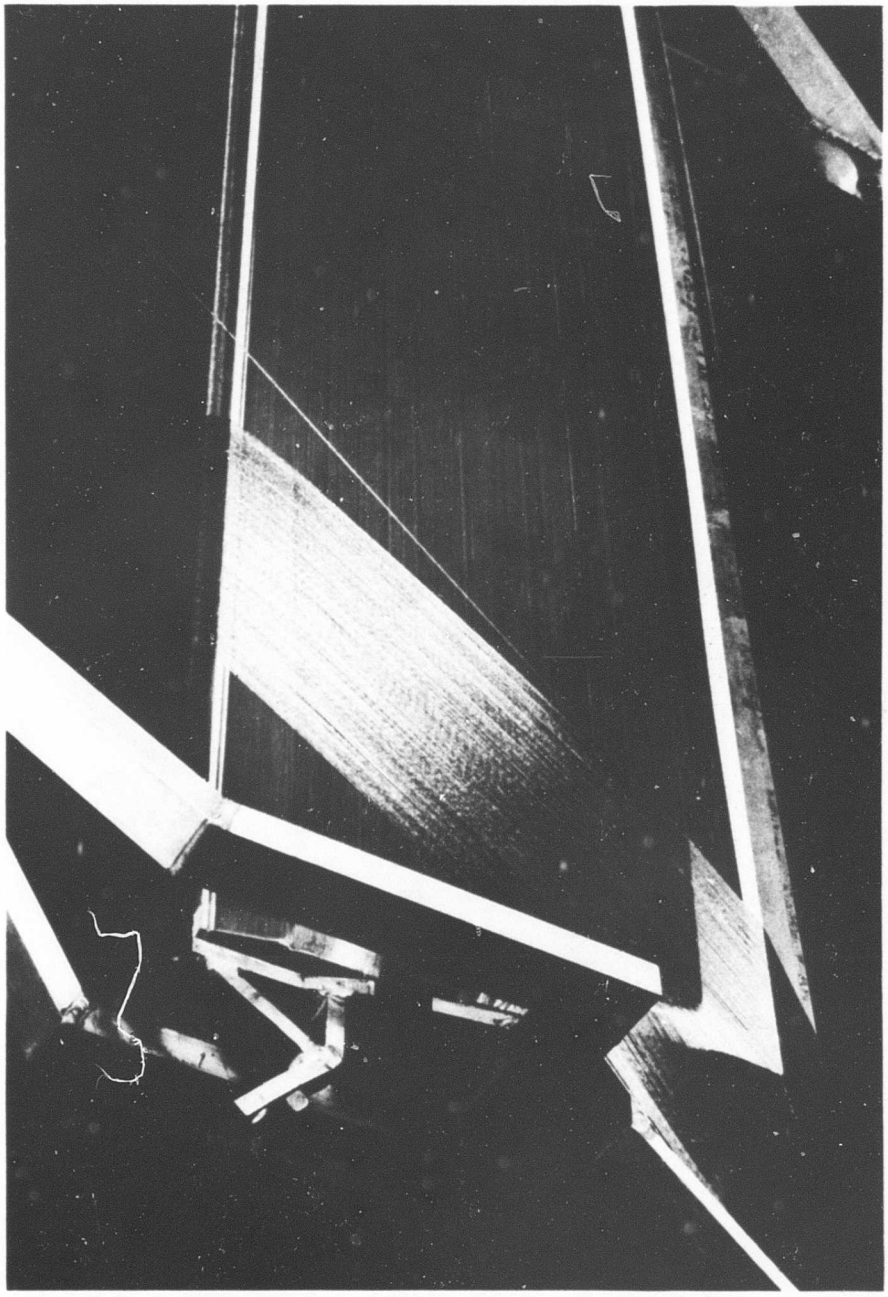

Figure 4. Winding First Layer of 45-Degree Fibers.

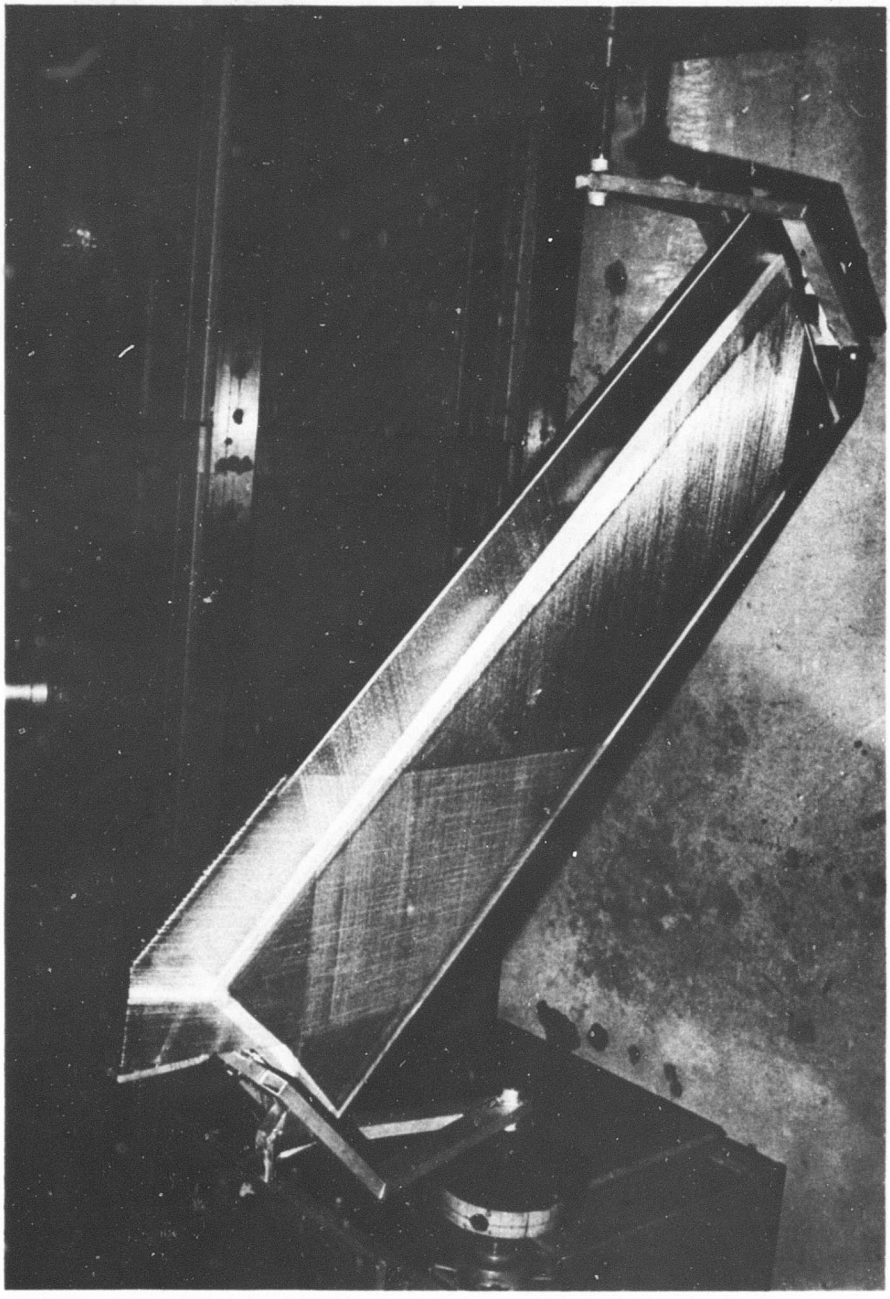

Figure 5. Winding Second Layer of 45-Degree Fibers.

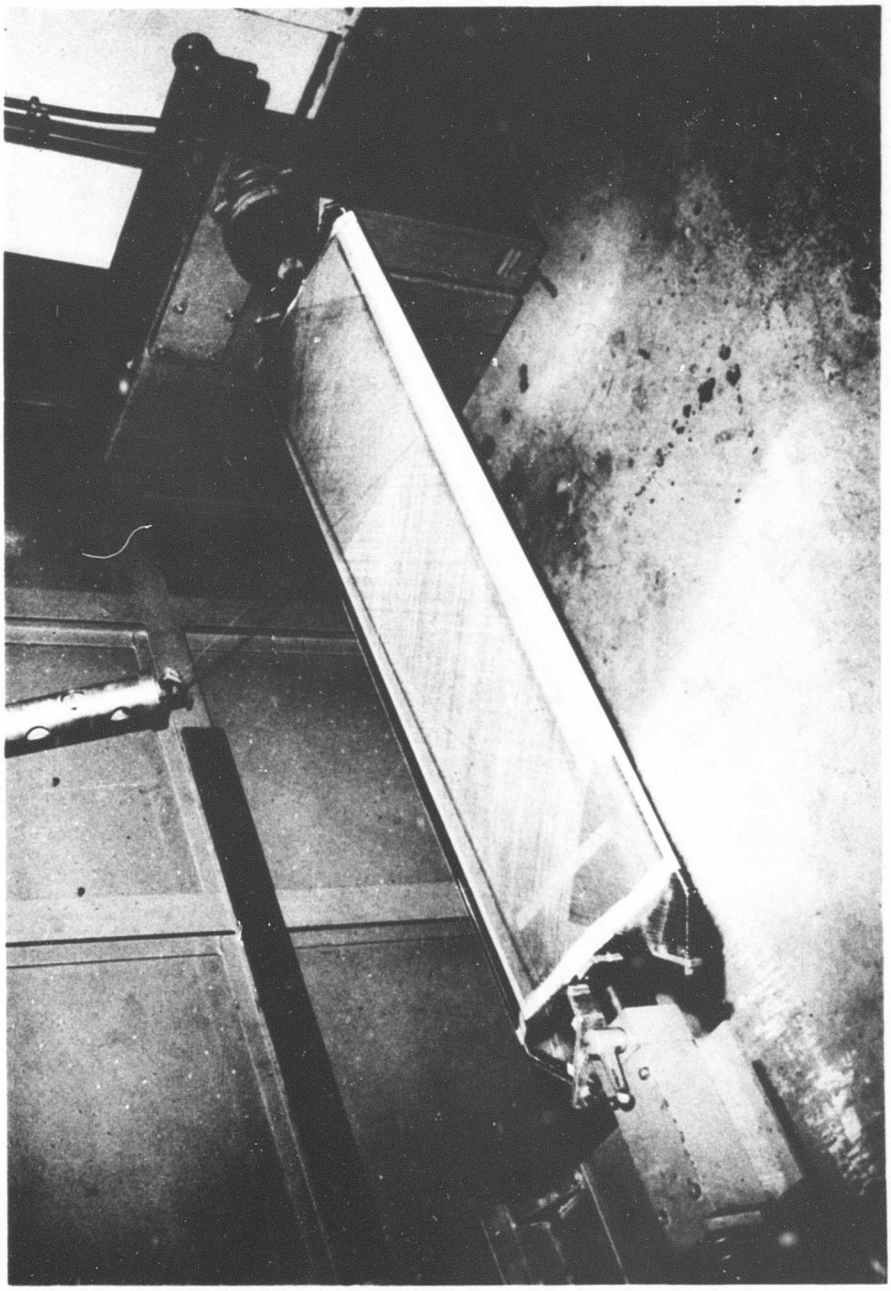

Figure 6. Winding Hoop Fibers.

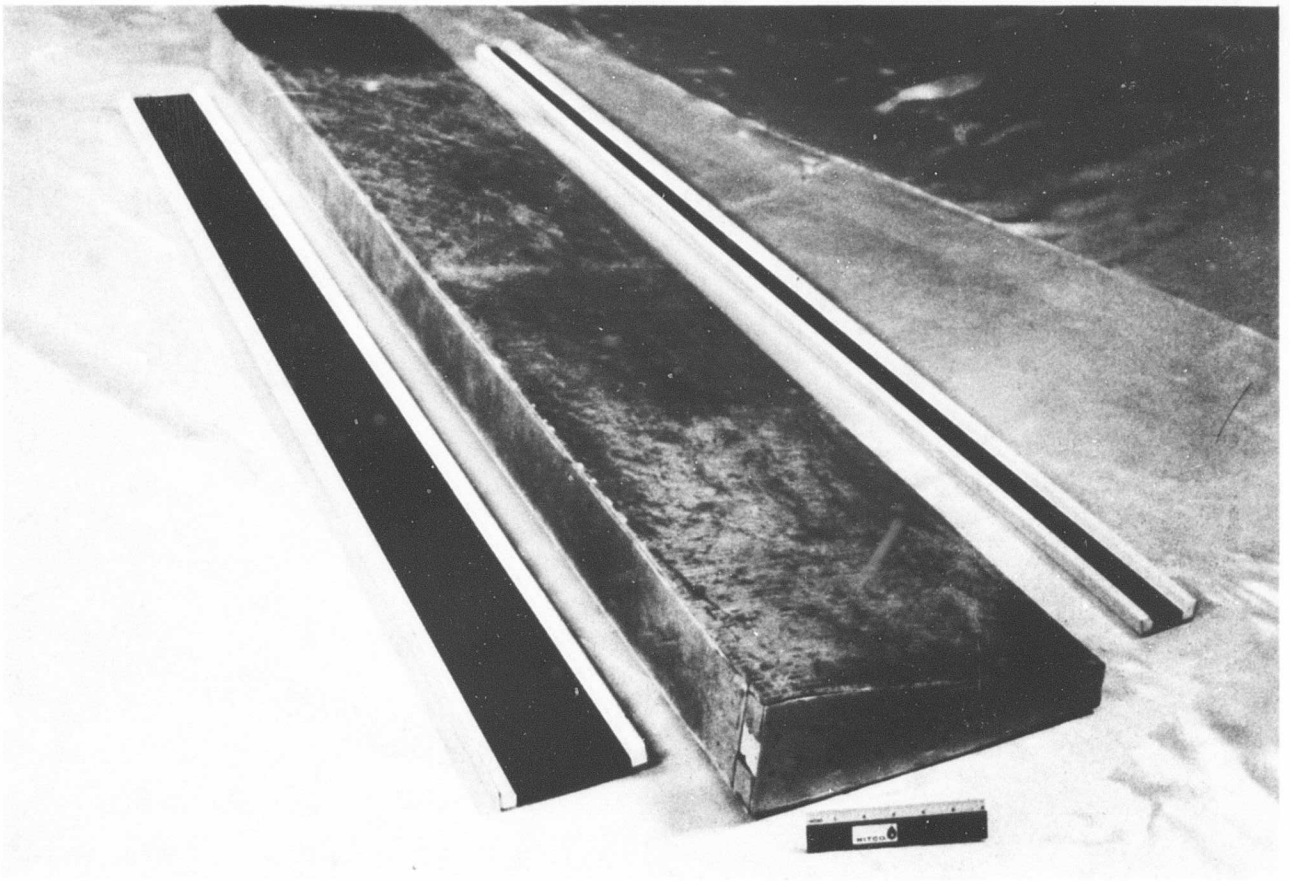

Figure 7. Prefabricated Spars and Completed Inside Face.

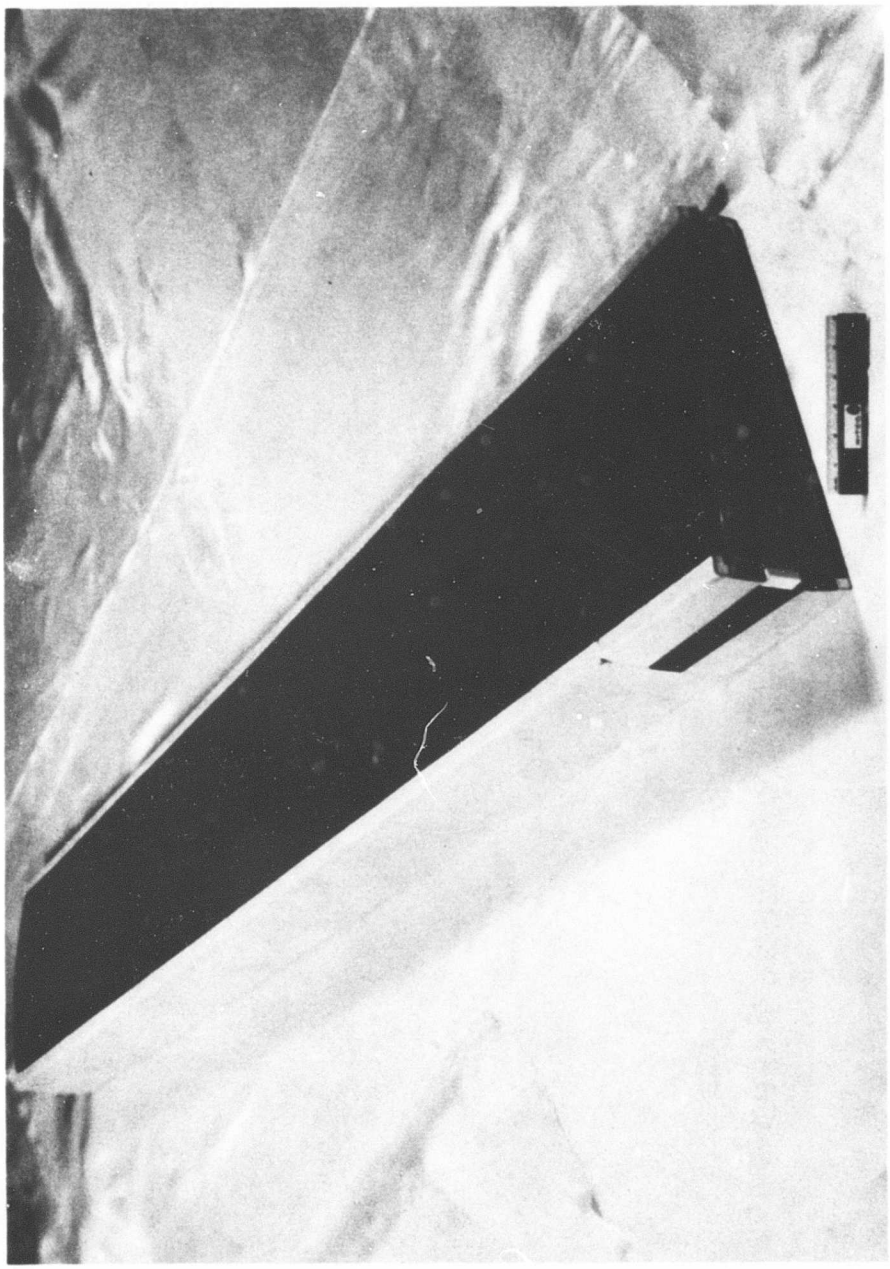

Figure 8. Inside Face With Spars and Honeycomb Assembled.

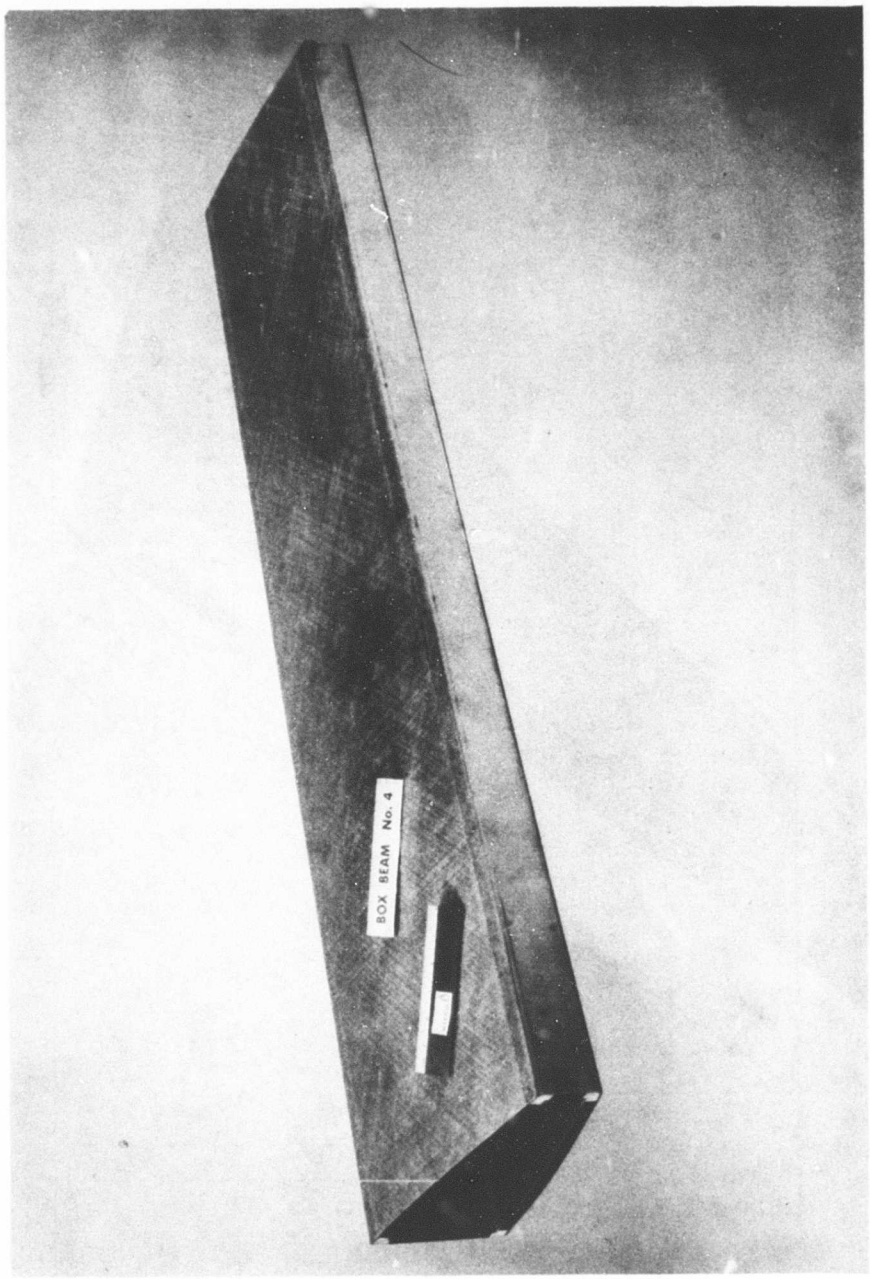

Figure 9. Box Beam After Trim.

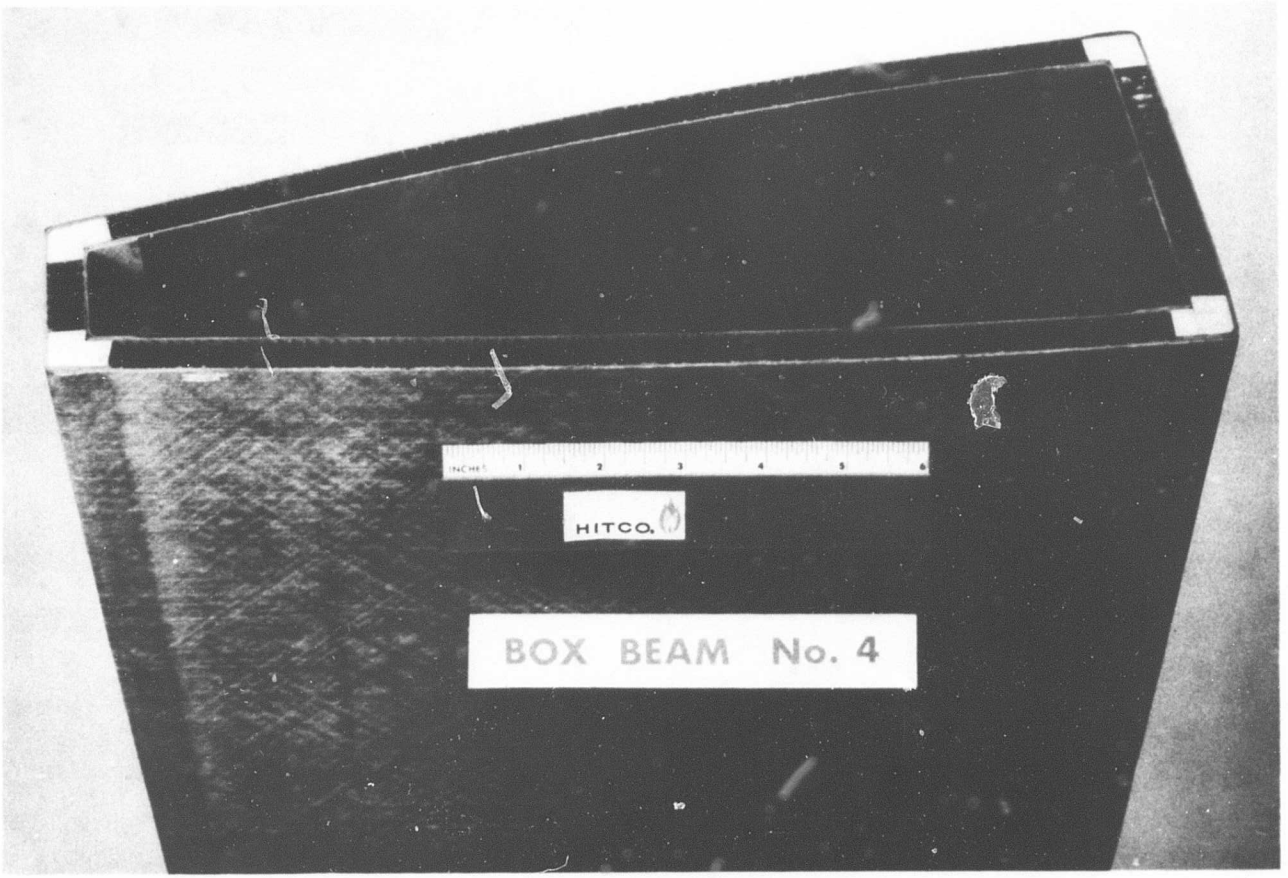

Figure 10. End View of Box Beam After Trim.

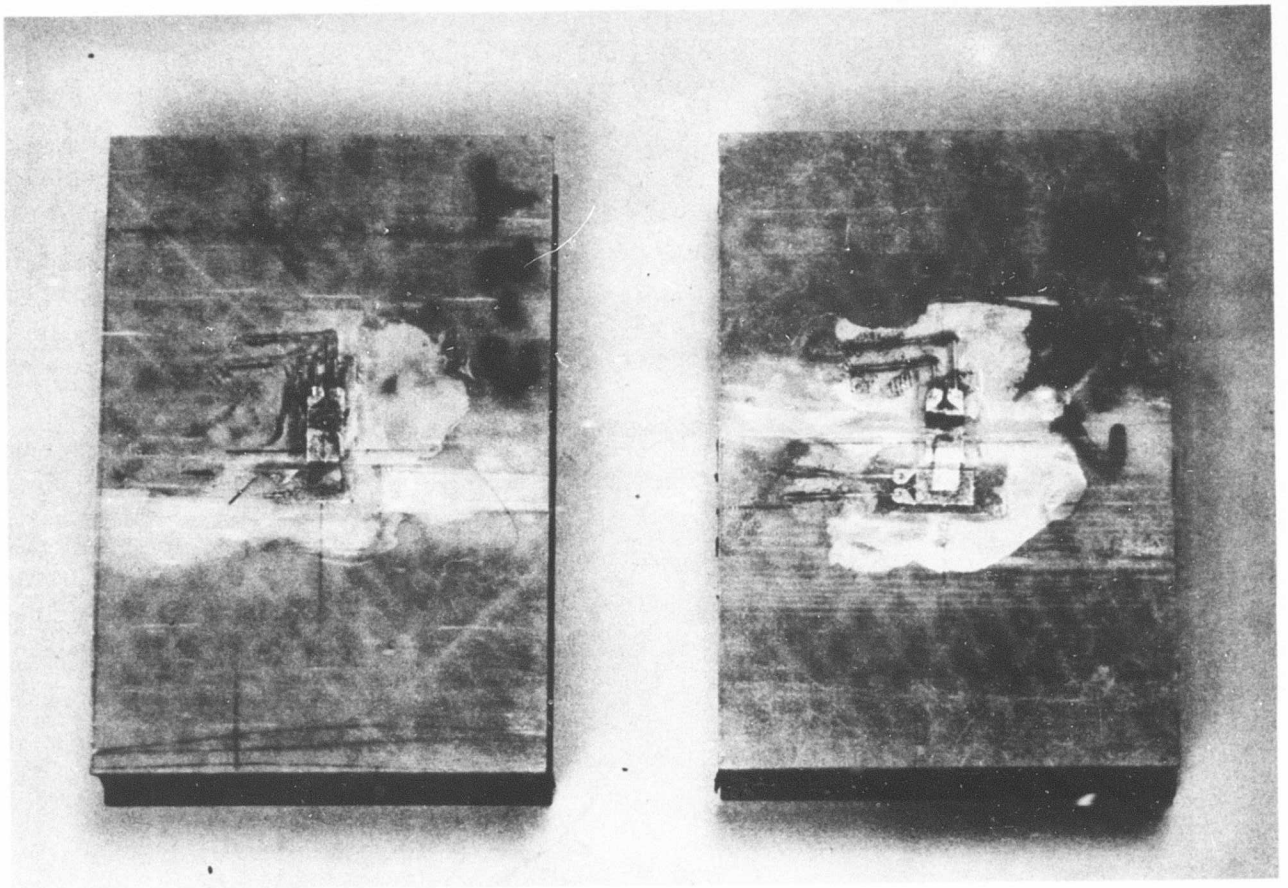

Figure 11. Edgewise Compression Specimens Showing Skin Failure.

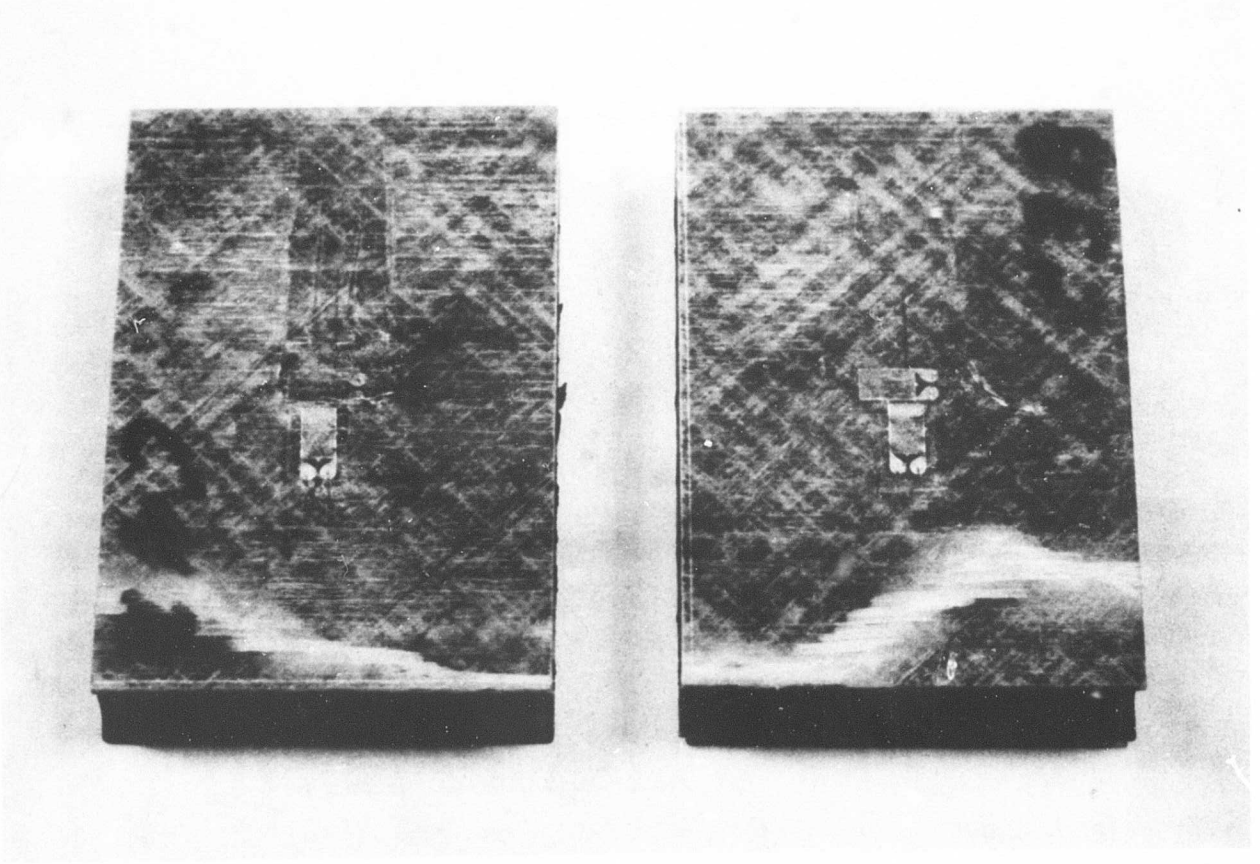

Figure 12. Edgewise Compression Specimens Showing Edge Failure.

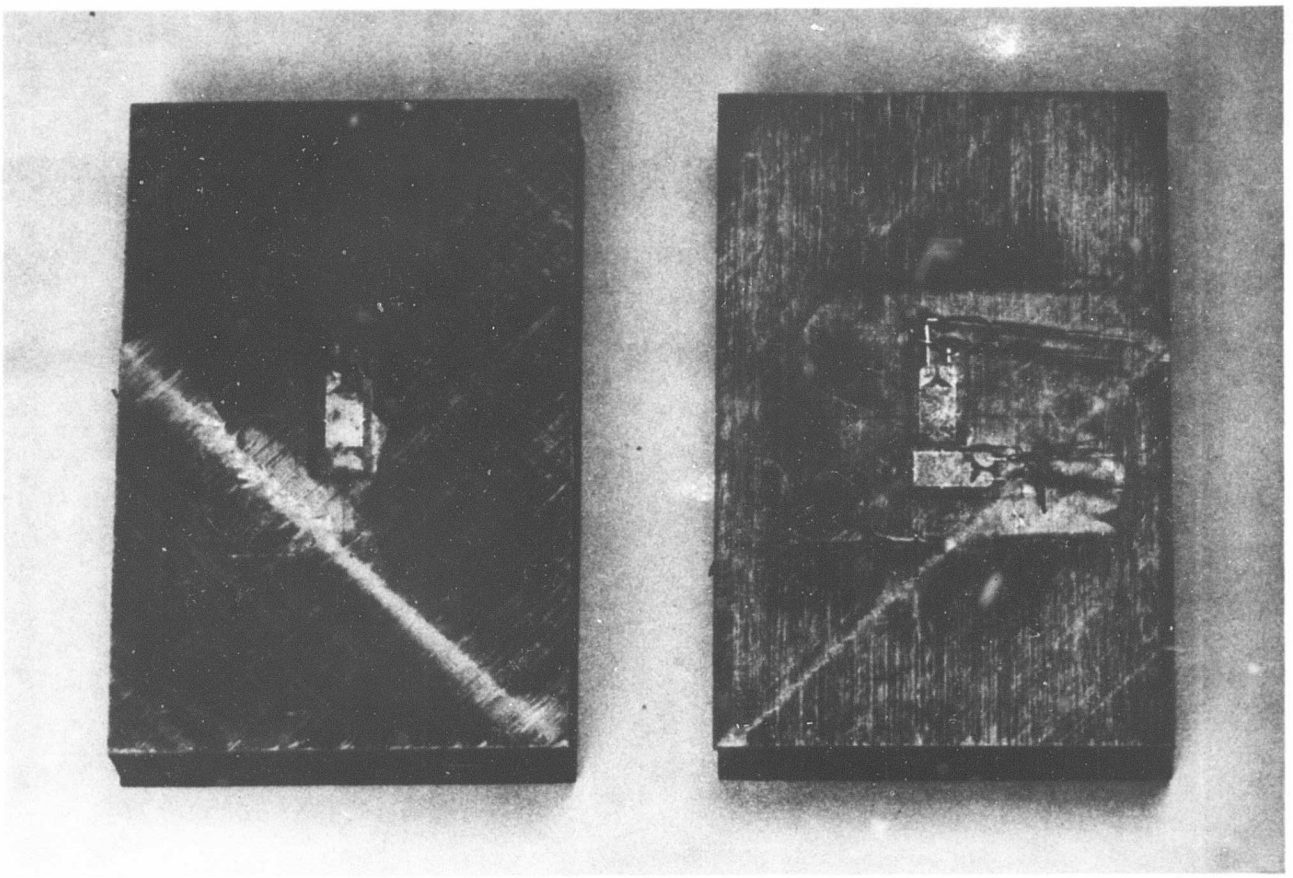

Figure 13. Edgewise Compression Specimens Showing Shear Failure.

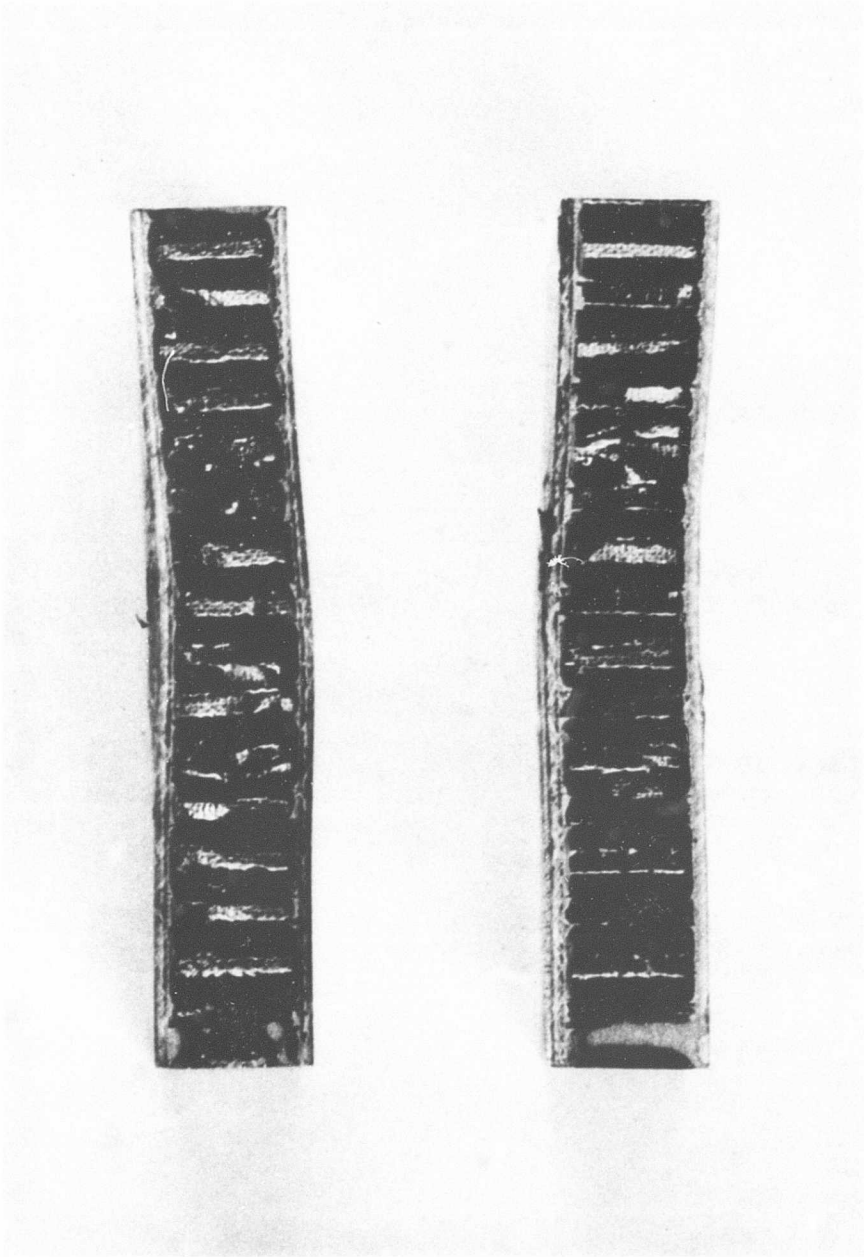

Figure 14. Edgewise Compression Specimens Showing Buckling Failure.

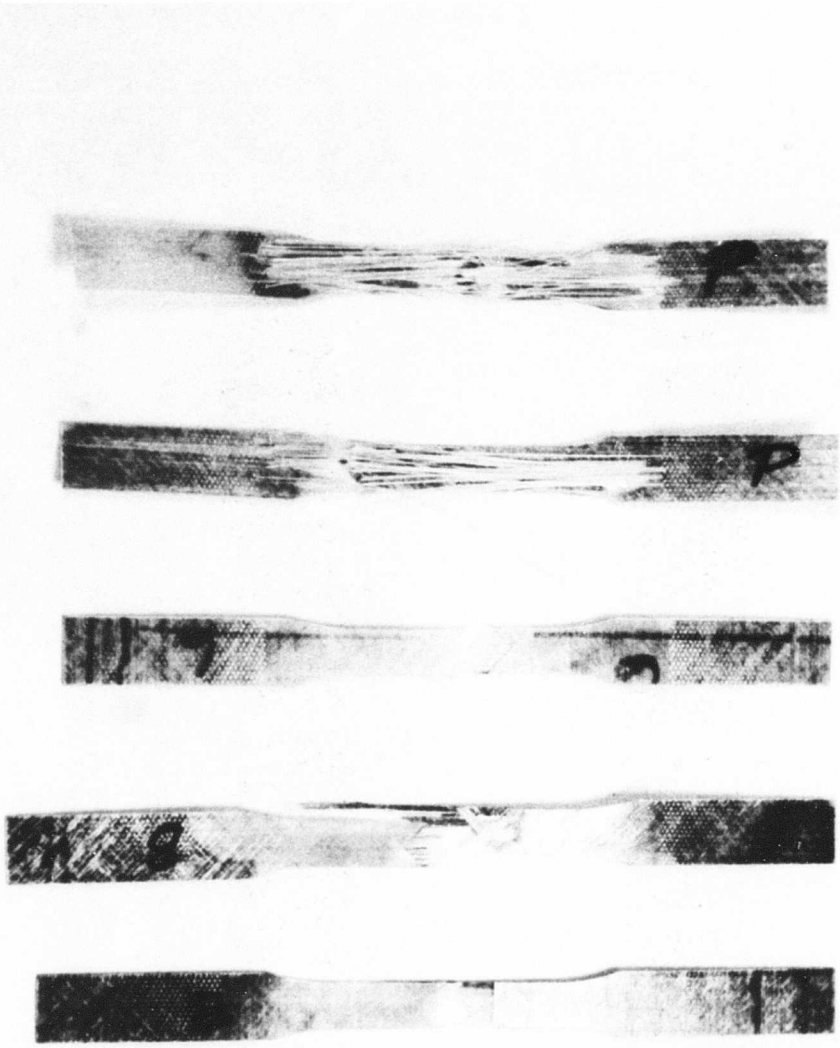

Figure 15. Laminate Tensile Specimens After Test, Box Beam No. 3.

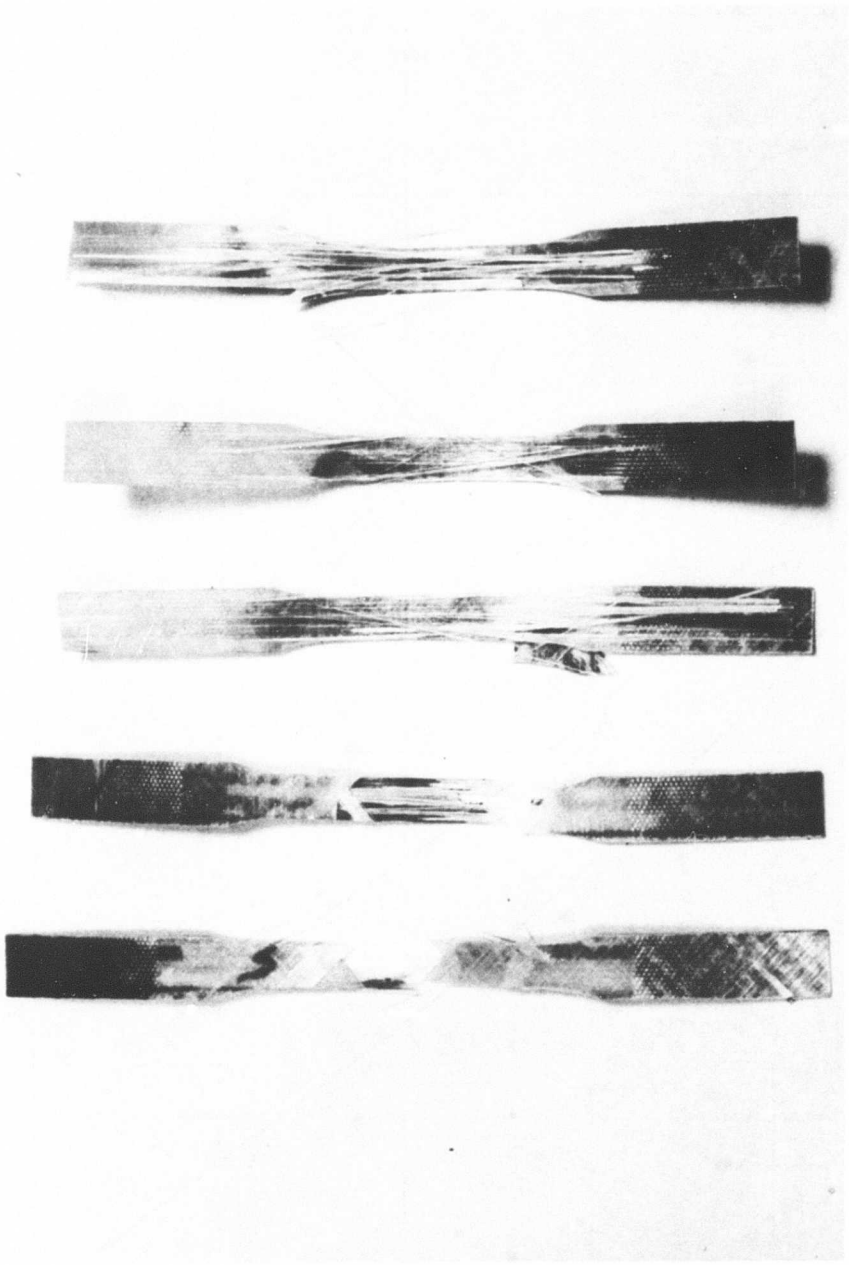

Figure 16. Laminate Tensile Specimens After Test, Box Beam No. 4.

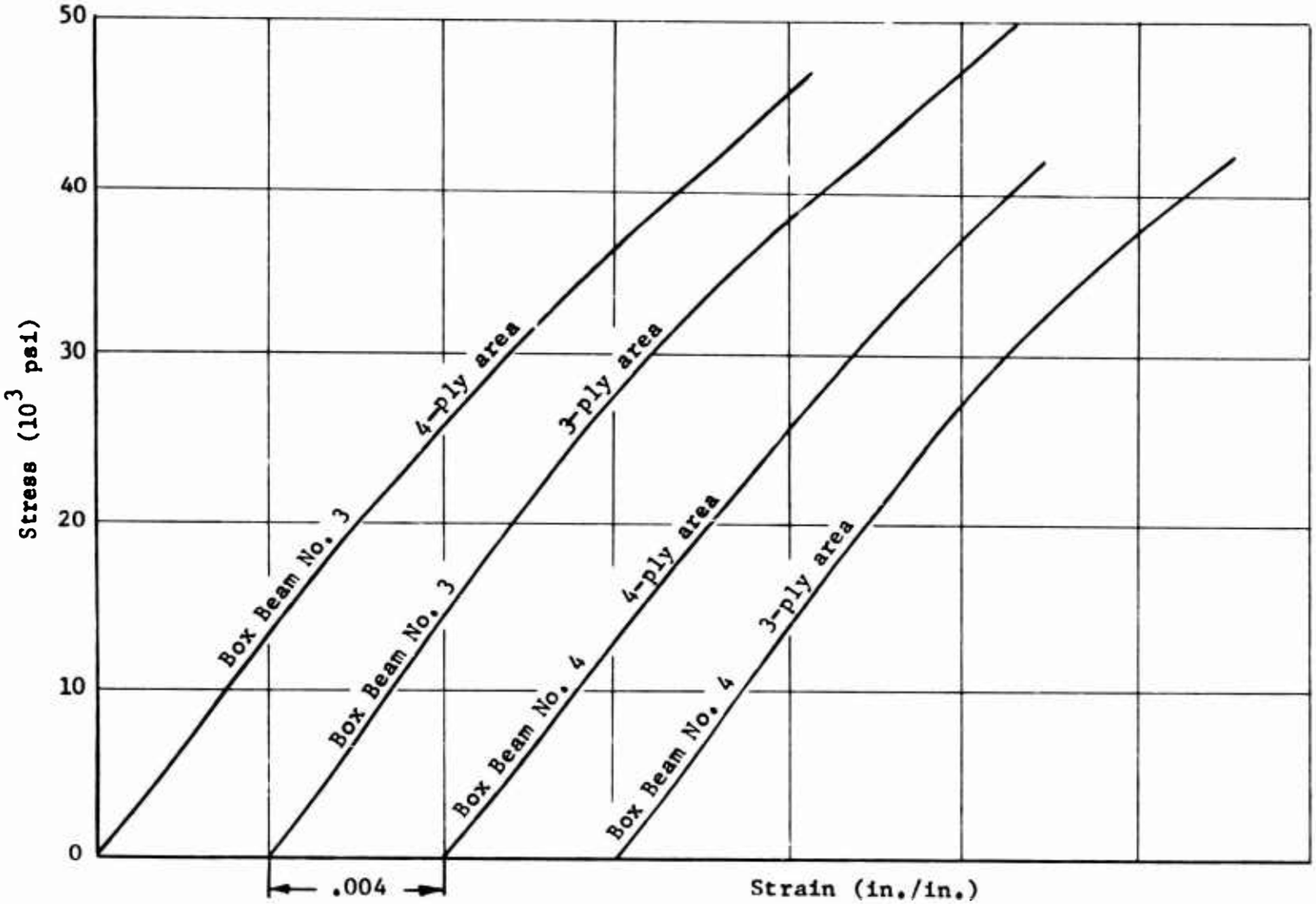

Figure 17. Typical Stress-Strain Curves, Edgewise Compression Specimens.

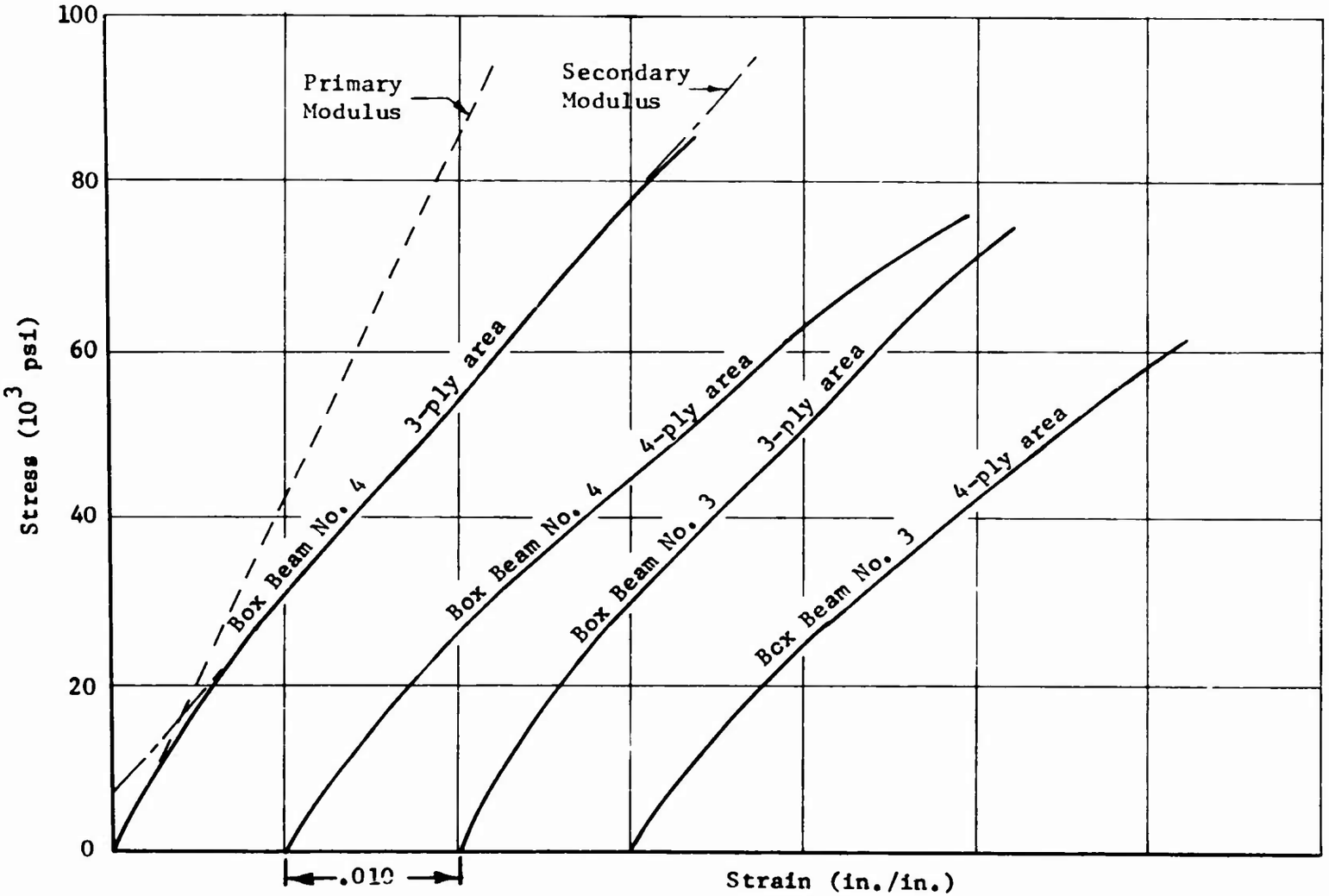

Figure 18. Typical Stress-Strain Curves, Laminate Tensile Specimens.

TABLE I
BOX BEAM FABRICATION SUMMARY

Beam No.	Fabrication Method	Material	Cure Pressure	Flange Weight (lb/ft^2)
1	Hand Lay-up	E-HTS/XP-251 (12 in.-wide tape) Metlbond 400 Adhesive HRP 3/16-GF 11-4.0 Core	Autoclave 50 psi	1.171
2	Filament Wound	E-HTS/E787 (20 end roving) Metlbond 329 Adhesive HRP 3/16-GF 11-4.0 Core	Vacuum Bag 5-10 psi	1.330
3	Filament Wound (Tailored Hoops)*	E-HTS/E787 (20 end roving) Metlbond 329 Adhesive HRP 3/16-GF 11-4.0 Core	Vacuum Bag 5-10 psi	1.323
4	Filament Wound (Tailored Hoops)*	S-HTS/E787 (20 end roving) Metlbond 329 Adhesive HRP 3/16-GF 11-4.0 Core	Vacuum Bag 5-10 psi	1.245
5 and 6	Filament Wound	E-HTS/E787 (20 end roving) Metlbond 329 Adhesive HRP 3/16-GF 11-4.0 Core	Vacuum Bag 5-10 psi	1.372 1.351

*The hoop fibers were discontinued at midbay on the part to give a tailoring effect.
All material was preimpregnated.
All spar faces were fabricated with E-HTS/XP-251 preimpregnated tape.

TABLE II
SANDWICH PANEL EVALUATION - FLATWISE TENSILE TESTS

Adhesive System	Specimen No.	Stress (psi)	Type Failure
Metlbond 329 Adhesive	1	873	Adhesive to Core
	2	914	Adhesive to Core
	3	909	Adhesive to Core
	4	884	Adhesive to Core
	5	853	Adhesive to Core
	6	959	Adhesive to Core
	Ave	899	
AF-110-A Adhesive	1	795	Adhesive to Core
	2	863	Adhesive to Core
	3	768	Adhesive to Core
	4	805	Adhesive to Core
	Ave	808	
Metlbond 500 Prepreg 181 Cloth (4 plies) (No XP-251 Faces)	1	800	Adhesive to Core
	2	945	Adhesive to Core
	3	1108	Adhesive to Core
	4	1000	Adhesive to Core
	Ave	963	
E-787 Resin 2 Plies Impregnated 120 Cloth	1	314	Adhesive to Core
	2	367	Adhesive to Core
	3	375	Adhesive to Core
	4	325	Adhesive to Core
	5	338	Adhesive to Core
	Ave	344	

Faces - XP-251-E unidirectional tape, 4 plies oriented at 0°, 45°, 90°, and 135°.
Core - HRP 3/16-GF 11-4.0, 0.46 inch thick.
Test Specification - MIL-STD-401A, 2.0-x-2.0-inch specimens.

TABLE III
PREPRODUCTION FABRICATION AND SETUP TIME

Item	Filament Wound Beam		Hand Lay-Up Beam	
	Men Reqd	Man-hrs.	Men Reqd	Man-hrs.
1. Fabricate Spar Faces	1	12	1	12
2. Prepare Mandrel (includes hardware changes for each ply on filament wound beam)	2	40	1	8
3. Set Up Winding Machine	2	15	-	-
4. Fab Inside Face	2	15	1	20
5. Bag and Cure	1	3	-	-
6. Trim	1	10	-	-
7. Position Honeycomb and Foam Corners	2	24	2	24
8. Bag and Cure	1	3	-	-
9. Trim	1	10	-	-
10. Fab Outside Face	2	15	1	20
11. Bag and Cure	1	3	1	3
12. Final Trim	1	15	1	15
Total Hours		165		102

TABLE IV
BOX BEAM NO. 1 - FLATWISE TENSILE SPECIMENS

Specimen No.	Type Failure	Failure Load (lbs)	Stress (psi)
T-1B*	Adhesive	1675	419
T-2B	Adhesive	1410	353
T-3B	Adhesive	1910	478
T-4B	Adhesive	1945	486
T-5B	Adhesive	1870	468
T-6B	Adhesive	1945	486
T-7B	Adhesive	1765	441
T-8B	Adhesive	1890	473
T-1T**	Adhesive	1700	425
T-2T	Adhesive	1715	429
T-3T	Adhesive	1990	498
T-4T	Adhesive	1785	446
T-5T	Adhesive	1435	359
T-6T	Adhesive	1840	460
T-7T	Adhesive	1785	446
T-8T	Adhesive	1970	493
		Average =	448
		Std Dev =	43.4

*Bottom flange
**Top flange
Glass - E-HTS
Resin - XP-251
Core - HRP 3/16-GF 11-4.0, 0.46 inch thick
Adhesive - Metlbond 400
Specimen Size - 2.0 x 2.0 inches
Test Specification - MIL-STD-401A
Facing Orientation - 4 plies at .010 inch/ply

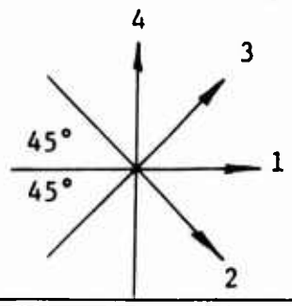

TABLE V
BOX BEAM NO. 1 - EDGEWISE COMPRESSION SPECIMENS

Specimen No.	Area ($in.^2$)	Failure Load (lbs)	Stress (psi)	Modulus (10^6 psi)	Poisson's Ratio
C-1T*	.16	6000	37,500	4.01	.370
C-2T	.16	5350	33,440	3.95	.356
C-3T	.16	5200	32,500	3.49	.368
C-4T	.16	5650	35,310	3.90	.392
C-5T	.16	5000	31,250	3.77	.362
C-1B**	.16	5390	33,690	4.20	.329
C-2B	.16	6000	37,500	4.11	.403
C-3B	.16	6300	39,380	3.90	.364
C-4B	.16	6200	38,750	3.87	.359
C-5B	.16	6000	37,500	3.63	.310
		Average =	35,680	3.88	.361
		Std Dev =	2,827	.21	.027

*Top flange
**Bottom flange
Glass - E-HTS
Resin - XP-251
Core - HRP 3/16-GF 11-4.0, 0.46 inch thick
Adhesive - Metlbond 400
Specimen Size - 3.0 x 2.0 inches
Test Specification - MIL-STD-401A
Facing Orientation - 4 plies at .010 inch/ply

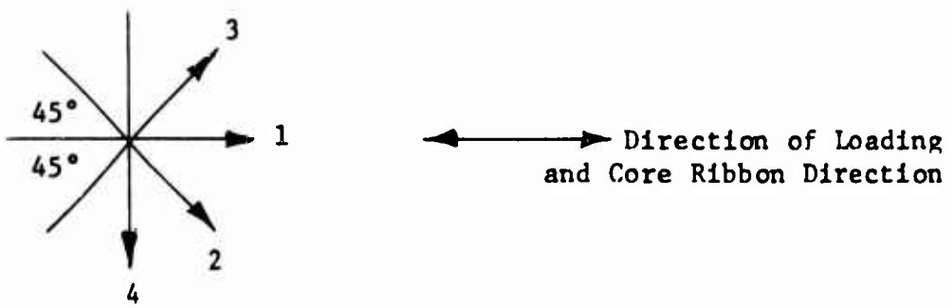

TABLE VI
BOX BEAM NO. 1 - LAMINATE TENSILE SPECIMENS

Specimen No.	Specimen Width (in.)	Specimen Thickness (in.)	Failure Load (lbs)	Stress (psi)	Primary Modulus (10^6 psi)	Secondary Modulus (10^6 psi)
LT1-TM	.502	.040	1075	53,536	3.25	1.72
LT2-TM	.504	.040	1080	53,571	3.01	1.65
LT3-TM	.510	.040	945	46,324	2.94	1.66
LT4-TM	.502	.040	990	49,303	3.09	1.53
LT1-TB	.507	.040	985	48,570	2.83	1.68
LT2-TB	.502	.040	840	41,833	2.50	1.31
LT3-TB	.501	.040	985	49,152	2.96	1.79
LT4-TB	.498	.040	960	48,193	3.08	1.79
LT1-BM	.498	.040	1030	51,707	3.08	1.70
LT2-BM	.[illegible]	.040	995	49,850	2.89	1.70
LT3-BM	[illegible]	.040	840	41,833	3.09	1.88
LT4-BM	.511	.040	870	42,564	2.66	1.62
LT1-BB	.508	.040	825	40,600	2.66	1.18
LT2-BB	.503	.040	785	39,016	2.69	1.63
LT3-BB	.497	.040	820	41,247	2.98	1.80
LT4-BB	.502	.040	850	42,415	2.87	1.73
			Average =	46,232	2.91	1.65
			Std Dev =	4,850	.201	.180

Specimen Identification:
- TM = Top flange, mandrel side
- TB = Top flange, bag side
- BM = Bottom flange, mandrel side
- BB = Bottom flange, bag side

Glass - E-HTS
Resin - XP-251
Test Specification - Type I, FTMB 406, Method 1011
Ply Orientation - 4 plies at .010 inch/ply

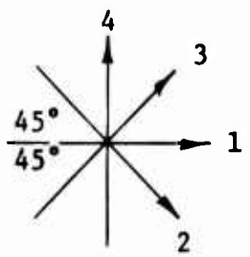

Direction of Loading and Core Ribbon Direction

TABLE VII
BOX BEAM NO. 2 - FLATWISE TENSILE SPECIMENS

Specimen No.	Type Failure	Failure Load (lbs)	Stress (psi)
T-1B*	Adhesive	4240	1060
T-2B	Adhesive	4440	1110
T-3B	Adhesive	3720	930
T-4B	External Bond	—	—
T-5B	Adhesive	3425	856
T-6B	Adhesive	3635	909
T-7B	Adhesive and Core	3755	939
T-8B	Adhesive	3600	900
T-1T**	Adhesive	4470	1118
T-2T	Adhesive	3760	940
T-3T	Adhesive	3680	920
T-4T	Adhesive	3865	966
T-5T	Adhesive	4175	1044
T-6T	Adhesive	3505	876
T-7T	Adhesive	3800	950
T-8T	Adhesive	4215	1054
		Average =	971
		Std Dev =	84

*Bottom flange
**Top flange
Glass - E-HTS
Resin - E-787
Core - HRP 3/16-GF 11-4.0, 0.46 inch thick
Adhesive - Metlbond 329
Specimen Size - 2.0 x 2.0 inches
Test Specification - MIL-STD-401A
Facing Orientation - 4 plies at approximately .010 inch/ply

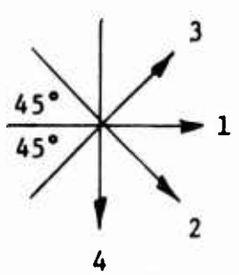

TABLE VIII
BOX BEAM NO. 2 - EDGEWISE COMPRESSION SPECIMENS

Specimen No.	Area ($in.^2$)	Failure Load (lbs)	Stress (psi)	Modulus (10^6 psi)	Poisson's Ratio
C-1T*	.188	8850	47,100	3.44	.392
C-2T	.188	7750	41,200	3.40	.370
C-3T	.188	7800	41,500	3.61	.474
C-4T	.188	10,000	53,200	3.27	.345
C-5T	.188	8450	44,900	3.56	.394
C-1B**	.188	8200	43,600	3.17	.370
C-2B	.188	8650	46,000	3.24	.344
C-3B	.188	9600	51,100	3.22	.372
C-4B	.188	9000	47,900	3.42	.388
C-5B	.188	9900	52,700	3.84	.357
		Average =	46,920	3.42	.381
		Std Dev =	4338	.21	.037

*Top flange
**Bottom flange
Glass - E-HTS
Resin - E-787
Core - HRP 3/16-GF 11-4.0, 0.46 inch thick
Adhesive - Metlbond 329
Specimen Size - 3.0 x 2.0
Test Specification - MIL-STD-401A
Facing Orientation - 4 plies at approximately .010 inch/ply

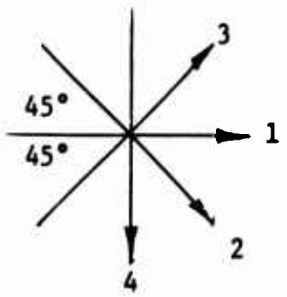

Direction of Loading and Core Ribbon Direction

TABLE IX
BOX BEAM NO. 2 - LAMINATE TENSILE SPECIMENS

Specimen No.	Specimen Width (in.)	Specimen Thickness (in.)	Failure Load (lbs)	Stress (psi)	Primary Modulus (10^6 psi)	Secondary Modulus (10^6 psi)
LT1-TM	.501	.046	1400	60,700	3.08	1.89
LT2-TM	.497	.047	1380	59,100	3.29	1.73
LT3-TM	.498	.048	1340	56,100	2.84	1.81
LT4-TM	.500	.048	1500	62,500	3.42	1.59
LT1-TB	.500	.046	1520	66,100	3.32	1.90
LT2-TB	.500	.046	1490	64,800	3.20	1.80
LT3-TB	.500	.046	1490	64,800	3.22	2.11
LT4-TB	.498	.046	1480	64,600	3.38	1.82
LT1-BM	.496	.046	1340	58,700	3.02	1.72
LT2-BM	.498	.047	1420	60,700	3.20	1.82
LT3-BM	.499	.048	1410	58,900	2.93	1.67
LT4-BM	.499	.048	1380	57,600	2.71	1.49
LT1-BB	.500	.047	1430	60,900	2.99	1.84
LT2-BB	.498	.047	1400	59,800	2.80	1.80
LT3-BB	.500	.046	1400	60,900	2.96	1.88
LT4-BB	.496	.047	1450	62,200	2.92	1.73
			Average =	61,150	3.08	1.79
			Std Dev =	2,848	.22	.14

Specimen Identification:
TM = Top flange, mandrel side
TB = Top flange, bag side
BM = Bottom flange, mandrel side
BB = Bottom flange, bag side
Glass - E-HTS
Resin - E-787
Test Specification - Type I, FTMB 406, Method 1011
Ply Orientation - 4 plies at .010 inch/ply

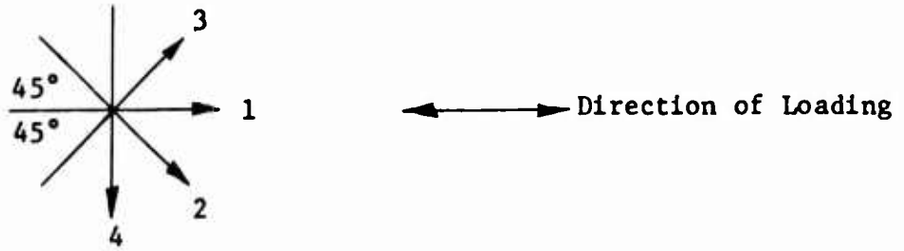

TABLE X
BOX BEAM NO. 3 - FLATWISE TENSILE SPECIMENS

Specimen No.	Type Failure	Failure Load (lbs)	Stress (psi)
T-1T*	Adhesive	3240	810
T-2T	External Bond	1725	431***
T-3T	Adhesive	3505	876
T-4T	Adhesive	2805	701
T-1B**	Adhesive	2975	744
T-2B	External Bond	1645	411***
T-3B	Adhesive	2940	735
T-4B	Adhesive	2760	690
T-5T	External Bond	2470	618***
T-6T	Adhesive	3235	809
T-7T	Adhesive	3100	775
T-8T	Adhesive	3310	827
T-5B	Face Failure	3390	848
T-6B	Adhesive	2210	553
T-7B	Face Failure	3715	929
T-8B	Adhesive	2620	655
		Average =	766
		Std Dev =	101

*Top flange
**Bottom flange
***Not included in average
Glass - E-HTS
Resin - E-787
Core - HRP 3/16-GF 11-4.0, 0.46 inch thick
Adhesive - Metlbond 329
Specimen Size - 2.0 x 2.0 inches
Test Specification - MIL-STD-401A

Facing Orientation

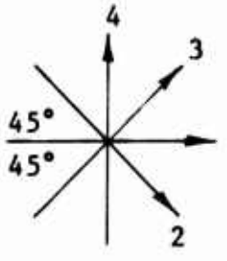

4 plies
Specimens
1 thru 4

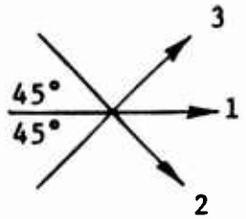

3 plies
Specimens 5 thru 8

TABLE XI
BOX BEAM NO. 3 - EDGEWISE COMPRESSION SPECIMENS

Specimen No.	Area ($in.^2$)	Failure Load (lbs)	Stress (psi)	Modulus (10^6 psi)	Poisson's Ratio
C-1T*	.193	8300	43,000	3.37	.308
C-2T	.193	8740	45,290	3.29	.323
C-3T	.192	8400	43,750	3.39	.374
C-1B**	.192	9900	51,560	3.33	.317
C-2B	.193	9200	47,670	3.40	.310
		Average =	46,254	3.36	.324
		Std Dev =	3,462	.046	.023
C-4T	.144	8100	56,250	3.49	.427
C-5T	.145	7180	49,520	3.51	.477
C-6T	.145	6980	48,140	3.41	.492
C-4B	.145	7200	49,660	3.46	.438
C-5B	.144	7800	54,170	3.45	.446
		Average =	51,548	3.46	.456
		Std Dev =	3,474	.038	.027

*Top flange
**Bottom flange
Glass - E-HTS
Resin - E-787
Core - HRP 3/16-GF 11-4.0, 0.46 inch thick
Adhesive - Metlbond 329
Specimen Size - 3.0 x 2.0 inches
Test Specification - MIL-STD-401A

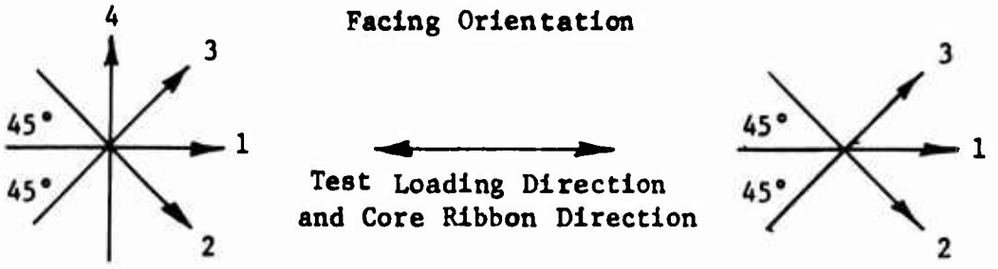

4 plies - 0.010 inch/ply
Specimens 1 thru 3

3 plies - 0.010 inch/ply
Specimens 4 thru 6

TABLE XII
BOX BEAM NO. 3 - LAMINATE TENSILE SPECIMENS

Specimen No.	Specimen Width (in.)	Specimen Thickness (in.)	Failure Load (lbs)	Stress (psi)	Primary Modulus (10^6 psi)	Secondary Modulus (10^6 psi)
LT1-TM	.501	.048	1350	56,130	3.08	1.80
LT2-TM	.502	.048	1340	55,600	3.02	1.53
LT1-TB	.503	.048	1520	62,970	3.26	1.96
LT2-TB	.502	.048	1500	62,240	3.11	1.70
LT1-BM	.502	.048	1360	56,430	3.22	1.88
LT2-BM	.500	.048	1390	57,920	3.11	1.72
LT1-BB	.502	.048	1525	63,280	3.02	1.83
LT2-BB	.501	.048	1410	58,630	3.15	1.80
			Average =	59,150	3.12	1.78
			Std Dev =	3,209	.09	.13
LT3-TM	.503	.036	1245	68,750	3.31	2.11
LT4-TM	.503	.036	1340	74,000	3.65	2.22
LT3-TB	.504	.036	1390	76,590	3.46	2.20
LT4-TB	.501	.036	1350	74,830	3.48	2.03
LT3-BM	.501	.036	1270	70,400	3.28	2.13
LT4-BM	.500	.036	1360	75,560	3.78	2.32
LT3-BB	.501	.036	1390	77,050	3.70	2.31
LT4-BB	.504	.036	1350	74,380	3.60	2.13
			Average =	73,945	3.53	2.18
			Std Dev =	2,924	.18	.10

Specimen Identification:
- TM = Top flange, mandrel side
- TB = Top flange, bag side
- BM = Bottom flange, mandrel side
- BB = Bottom flange, bag side

Glass - E-HTS
Resin - E-787
Test Specification - Type I, FTMB 406, Method 1011

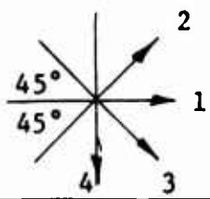

Loading Direction

4 plies
Specimens 1 & 2

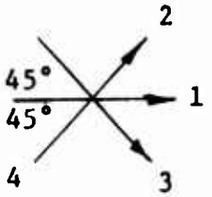

3 plies
Specimens 3 & 4

TABLE XIII
BOX BEAM NO. 4 - FLATWISE TENSILE SPECIMENS

Specimen No.	Type Failure	Failure Load (lbs)	Stress (psi)
T-1T*	Adhesive	3790	948
T-2T	Adhesive	3555	889
T-3T	Adhesive	3935	934
T-4T	Adhesive	3940	935
T-1B**	Adhesive	4075	1019
T-2B	Adhesive	3710	923
T-3B	Adhesive	3860	965
T-4B	Adhesive	4150	1038
T-5T	Adhesive	3735	934
T-6T	Face	3570	893
T-7T	Face	2520	630
T-8T	Adhesive	4010	1003
T-5B	Adhesive	3950	988
T-6B	Core and Face	3850	963
T-7B	Face	3500	875
T-8B	Adhesive	3875	969
		Average =	932
		Std Dev =	93

*Top flange
**Bottom Flange
Glass - S-HTS
Resin - E-787
Core - HRP 3/16-GF 11-4.0, 0.46 inch thick
Adhesive - Metlbond 329
Specimen Size - 2.0 x 2.0 inches
Test Specification - MIL-STD-401A

Facing Orientation

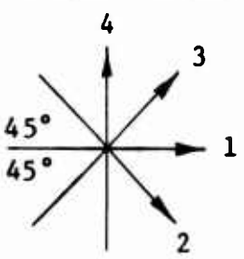

4 plies
Specimens
1 thru 4

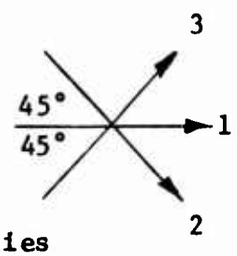

3 plies
Specimens 5 thru 8

TABLE XIV
BOX BEAM NO. 4 - EDGEWISE COMPRESSION SPECIMENS

Specimen No.	Area ($in.^2$)	Failure Load (lbs)	Stress (psi)	Modulus (10^6 psi)	Poisson's Ratio
C-1T*	.192	8400	43,750	3.50	.260
C-2T	.192	7900	41,150	3.65	.309
C-3T	.192	8400	43,750	3.65	.316
C-1B**	.192	9150	47,660	3.26	.273
C-2B	.192	8260	43,020	3.67	.301
		Average =	43,870	3.55	.292
		Std Dev =	2,370	.17	.024
C-4T	.144	7200	50,000	3.78	.402
C-5T	.145	7000	48,280	3.88	.433
C-6T	.145	8200	56,550	3.52	.429
C-4B	.144	7580	52,640	3.95	.404
C-5B	.144	6930	48,130	3.63	.450
		Average =	51,130	3.75	.424
		Std Dev =	3,540	.18	.020

*Top flange
**Bottom flange
Glass - S-HTS
Resin - E787
Core - HRP 3/16-GF 11-4.0, 0.46 inch thick
Adhesive - Metlbond 329
Specimen Size - 3.0 x 2.0 inches
Test Specification - MIL-STD-401A

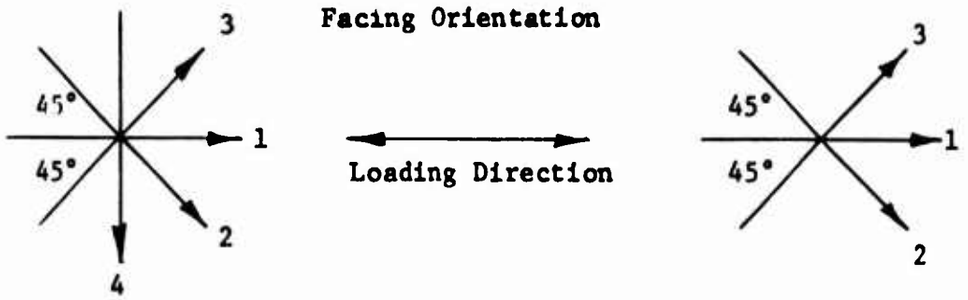

4 plies
Specimens 1,2, & 3

3 plies
Specimens 4,5, & 6

TABLE XV
BOX BEAM NO. 4 - LAMINATE TENSILE SPECIMENS

Specimen No.	Specimen Width (in.)	Specimen Thickness (in.)	Failure Load (lbs)	Stress (psi)	Primary Modulus (10^6 psi)	Secondary Modulus (10^6 psi)
LT1-TM	.499	.048	1590	66,390	3.49	1.89
LT2-TM	.501	.048	1530	63,620	3.36	1.95
LT1-TB	.501	.048	1860	77,340	3.48	1.78
LT2-TB	.500	.048	1950	81,250	3.29	1.89
LT1-BM	.500	.048	1660	69,170	3.50	1.75
LT2-BM	.500	.048	1550	64,580	3.34	1.91
LT1-BB	.502	.048	1820	75,520	3.34	2.39
LT2-BB	.504	.048	1750	72,340	3.33	2.03
			Average =	71,276	3.39	1.95
			Std Dev =	6,405	.08	.20
LT3-TM	.502	.036	1580	87,440	4.03	2.30
LT4-TM	.500	.036	1570	87,220	4.06	2.37
LT3-TB	.501	.036	2000	110,860	4.20	2.50
LT4-TB	.502	.036	1910	105,700	4.12	2.40
LT3-BM	.500	.036	1510	83,890	4.11	2.50
LT4-BM	.502	.036	1430	79,140	4.04	2.30
LT3-BB	.503	.036	2000	110,440	4.45	2.80
LT4-BB	.503	.036	1850	102,150	4.04	2.50
			Average =	95,850	4.13	2.46
			Std Dev =	12,770	.14	.16

Specimen Identification:
- TM = Top flange, mandrel side
- TB = Top flange, bag side
- BM = Bottom flange, mandrel side
- BB = Bottom flange, bag side

Glass - S-HTS
Resin - E-787
Test Specification - Type I, FTMB 406, Method 1011

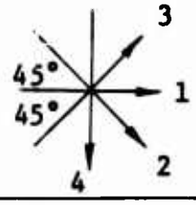

Loading Direction

4 plies
Specimens 1 & 2

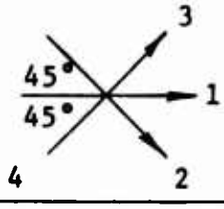

3 plies
Specimens 3 & 4

TABLE XVI
SUMMARY OF TEST RESULTS

Beam No.	Flatwise Tensile Strength (psi)	Edgewise Compression			Laminate Tensile			Resin Content % Wt.
		Strength (psi)	Modulus (10^6 psi)	Poisson's Ratio	Strength (psi)	Primary Modulus (10^6 psi)	Secondary Modulus (10^6 psi)	
1*	448	35,680	3.88	.361	46,232	2.91	1.65	19.6
2**	971	46,920	3.42	.381	61,150	3.08	1.79	23.4
3** (4-ply area)	766	46,254	3.36	.324	59,150	3.12	1.78	21.5
4*** (4-ply area)	932	43,870	3.55	.292	71,276	3.39	1.95	20.4
3** (3-ply area)	766	51,548	3.46	.456	73,945	3.53	2.18	21.5
4*** (3-ply area)	932	51,130	3.75	.424	95,850	4.13	2.46	20.4

*Hand lay-up, E-HTS/XP-251
**Filament wound, E-HTS/E787
***Filament wound, S-HTS/E787

CONCLUSIONS

The following conclusions can be drawn from the results obtained on this program:

1. The feasibility of filament winding the main load-carrying skin panels of an irregular contoured box beam wing structure has been demonstrated. Techniques have been developed to position and secure the fibers in the most optimum structural orientation even though these desired orientations are not ussually stable winding patterns.

2. The filament wound sandwich panels developed higher tensile strength and moduli than were obtained for the same panels using the hand lay-up technique.

3. The filament wound sandwich panel technique was more expensive in this program using developmental tooling than was the comparable hand lay-up technique. This was primarily caused by the additional setup time and cure stages required.

4. A good surface finish can be obtained using either the filament wound or hand lay-up techniques. Caul sheets capable of conforming to the wing contour are required.

5. An excellent core-to-face sandwich panel bond can be obtained by the utilization of a secondary adhesive system. Attempts to develop a primary bond using the preimpregnated nonwoven facing resin were unsuccessful because of insufficient flow. The use of a secondary adhesive system also eliminated the problem of resin drainage into the honeycomb cells. The adhesive selected formed excellent fillets and produced very good flatwise tensile strengths.

6. The incorporation of S-HTS glass filaments instead of E-HTS glass filaments results in higher tensile strength and tensile and compressive moduli as anticipated. The additional stiffness is helpful in reducing both spanwise and chordwise bending deflections.

7. All facing tensile and compressive strength values are felt to be conservative because of the inadequacy of the standard FTMS 406 and MIL-STD-401A test methods used. When test coupons contain 45-degree oriented fibers which terminate at cut edges a true strength test is difficult to obtain. A limited effort to develop a more suitable specimen configuration was expended; however, the additional cost involved restricted its usage in this program.

8. Face thickness tailoring can be accomplished to a limited degree. The amount of tailoring that can be accomplished will depend upon the induced stress distribution and the number of face plies available to tailor.

RECOMMENDATIONS

1. Evaluation of the process techniques developed in this program should be continued and extended to a full box beam structural test phase. Both scale and full-scale models should be structurally tested statically and in fatigue to demonstrate the structural integrity of the concepts developed.

2. Utilizing new tooling, a series of identical models should be fabricated and tested to evaluate further the consistency that can be obtained and expected from the materials and process techniques developed.

3. Additional work should be expended to develop more suitable coupon test methods for evaluating composites containing fibers oriented at 45-degree and similar off-warp directions.

4. Additional structural problems such as closing rib attachment, end fitting attachment, leading and trailing edge attachment, local inserts for span and skin panel attachments, core joints, and skin splices should be investigated in detail to develop structural concepts for incorporation into an actual reinforced plastic wing structure.

BIBLIOGRAPHY

1. Kimel, W. R., Elastic Buckling of a Simply Supported Rectangular Sandwich Panel Subjected to Combined Edgewise Bending Compression and Shear, No. 1859, Forest Products Laboratory, Madison, Wisconsin, November 1956.

2. Kuenzi, E. W., Norris, C. B., Jenkinson, P. M., Buckling Coefficients for Simply Supported and Clamped Flat, Rectanfular Sandwich Panels Under Edgewise Compression, No. 070, Forest Products Laboratory, Madison, Wisconsin, December 1964.

3. March, h. W., Effects of Shear Deformation in the Core of a Flat Rectangular Sandwich Panel, No. 1583, Forest Products Laboratory, Madison, Wisconsin, August 1955.

4. Peery, David J., Aircraft Structures, McGraw-Hill Book Co., New York, New York, 1950.

5. Shanley, F. R., Strength of Materials, McGraw-Hill Book Co., New York, New York, 1957.

6. Strength of Metal Aircraft Elements, MIL-HDBK-5, March 1961.

7. Tsai, Steven W., Structural Behavior of Composite Materials, NASA CR-71, Philco Corporation, Newport Beach, California, July 1964.

DISTRIBUTION

US Army Materiel Command	4
US Army Aviation Materiel Command	3
US Army Forces Southern Command	1
Chief of R&D, DA	2
US Army Aviation Materiel Laboratories	24
US Army Engineer R&D Laboratories	2
US Army Limited War Laboratory	1
US Army Research Office-Durham	1
US Army Test and Evaluation Command	1
Plastics Technical Evaluation Center	1
US Army Medical R&D Command	1
US Army Engineer Waterways Experiment Station	1
US Army Aviation School	1
US Army Infantry Center	2
US Army Tank-Automotive Center	2
US Army Aviation Maintenance Center	2
US Army Aviation Test Board	2
US Army Electronics Command	2
US Army Aviation Test Activity, Edwards AFB	2
Air Force Flight Test Center, Edwards AFB	2
US Army Field Office, AFSC, Andrews AFB	1
Systems Engineering Group (RTD), Wright-Patterson AFB	2
Naval Air Systems Command	6
Chief of Naval Research	1
US Naval Research Laboratory	1
US Naval Air Station, Norfolk	1
David Taylor Model Basin	1
Commandant of the Marine Corps	1
Marine Corps Liaison Officer, US Army Transportation School	1
Ames Research Center, NASA	1
Lewis Research Center, NASA	1
NASA Scientific and Technical Information Facility	2
NAFEC Library (FAA)	2
National Tillage Machinery Laboratory	1
US Army Board for Aviation Accident Research	1
Bureau of Safety, Civil Aeronautics Board	2
US Naval Aviation Safety Center, Norfolk	1
Federal Aviation Agency, Washington, D. C.	1
Civil Aeromedical Research Institute, FAA	2
The Surgeon General	1
Director of Defense Research and Engineering	1
US Army Ballistic Research Laboratories	1
US Army Materials Research Agency	1
Defense Documentation Center	20
US Government Printing Office	1

APPENDIX I
STRESS AND DEFLECTION ANALYSIS

The primary load-carrying structure of an NACA 64_2-215 airfoil, light aircraft wing was designed as a sandwich-wall box beam having E-HTS fiber glass reinforced plastic faces and a honeycomb core. Included in this appendix are the basic design loads, material properties, safety margins, and a stress and deflection analysis of the structure. The stress analysis includes primary bending stresses, shear stresses, and bending stresses due to secondary loading.

BASIC LOADS

The design loads on the NACA 64_2-215 airfoil are for maneuvering flight condition "A" as shown on Figure 19. The load factors for this condition are:

Design airspeed	=	175 mph
Aircraft load factor	=	8.00
Wing load factor - vertical direction	=	7.69
Wing load factor - aft direction	=	1.66

A factor of safety of 1.5 is applied to these loads for design purposes. The flight envelope and sign convention for the moments and shears are shown in Figures 19 and 20. The design moments, shears, and torsion versus wing station are shown in Figures 21, 22, and 23 for maneuvering flight condition "A". From the wing configuration, shown in Figure 24, it is noted that the structural portion of the airfoil section is between 35 percent and 75 percent of chord. All the analyses are based on this section of the wing.

The section properties versus wing station for the structural portion of the wing are shown in Figures 25 and 26.

MATERIAL DESIGN ALLOWABLES

The material properties for "E" glass were theoretically determined using the equations shown in Reference 7. Following is the input data required:

$E_g = 10.5 \times 10^6$ psi

$E_r = .6 \times 10^6$ psi

$\mu_g = .22$

$\mu_r = .35$

$V_r = .38$

$C = .20$

$K = 1.0$

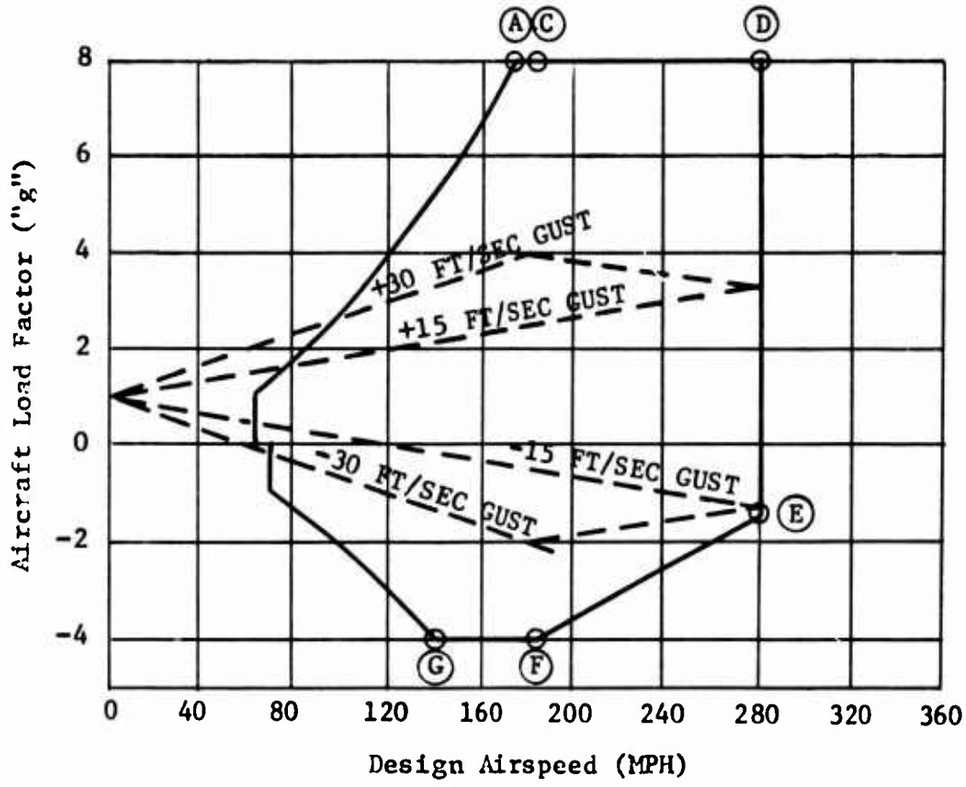

Figure 19. Aircraft Flight Envelope.

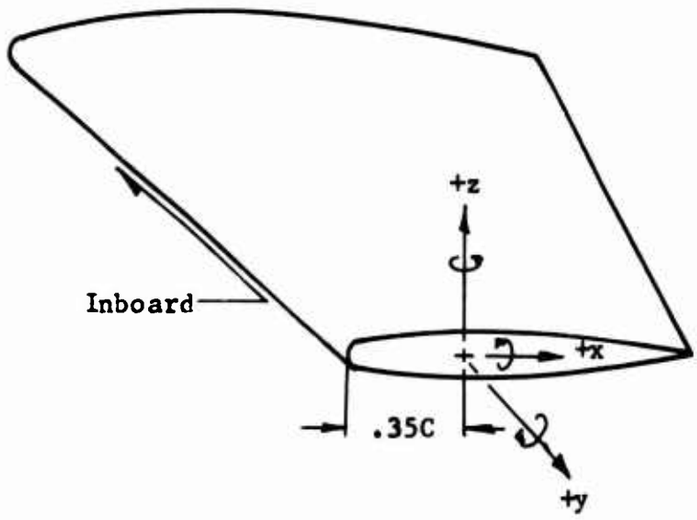

NOTE: "x" and "z" moments are positive when they produce compressive stresses in the wing where "x" and "z" are positive.

"y" moment is positive for nose up rotation.

Figure 20. Wing Sign Convention.

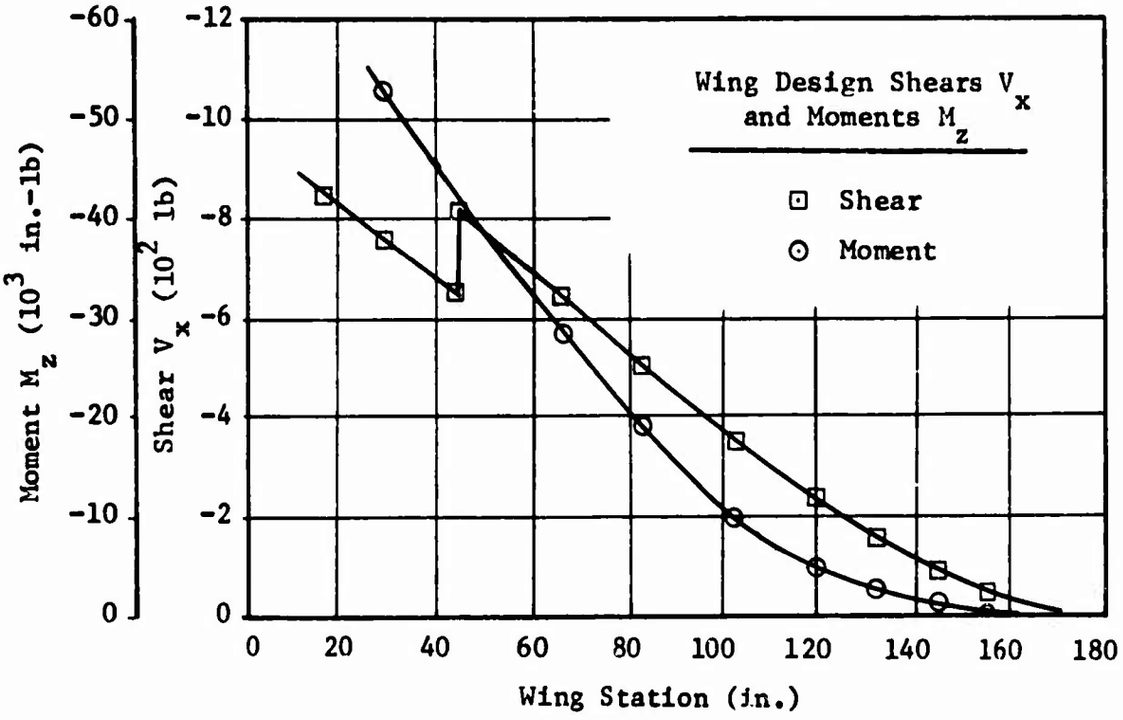

Figure 21. Wing Design Shears V_x and Moments M_z.

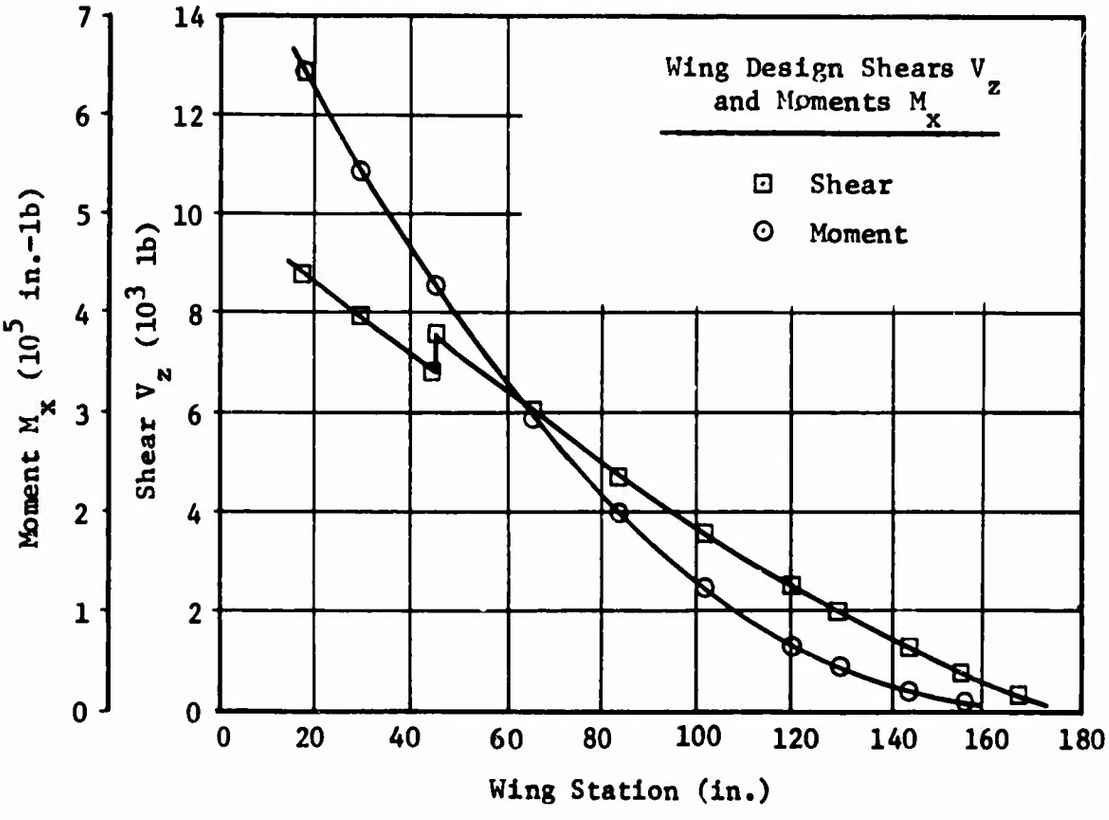

Figure 22. Wing Design Shears V_z and Moments M_x.

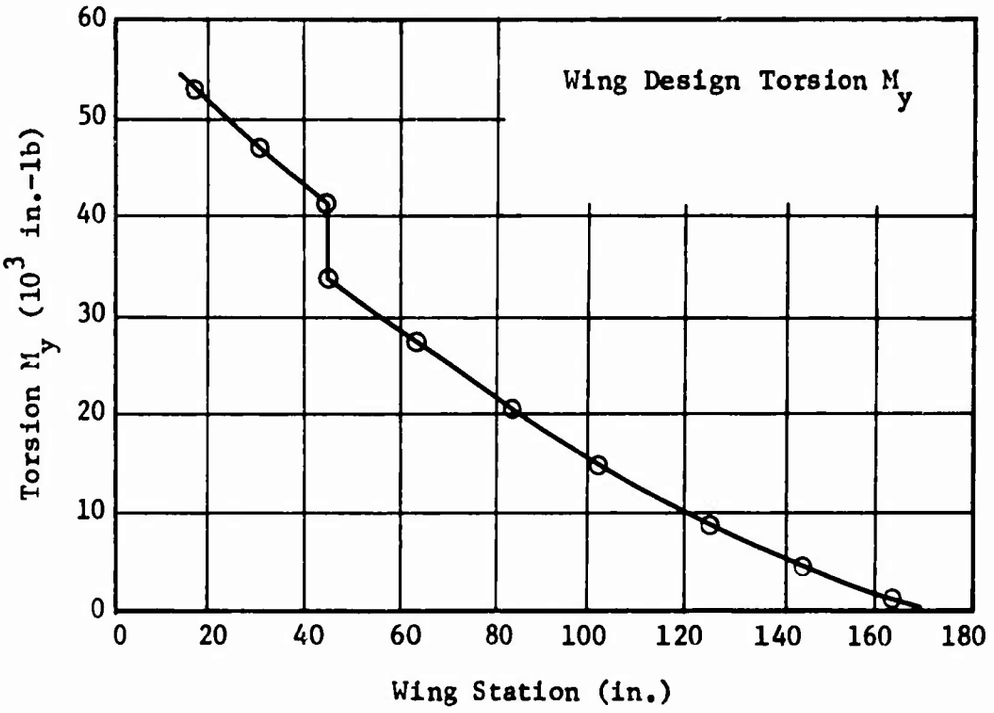

Figure 23. Wing Design Torsion M_y.

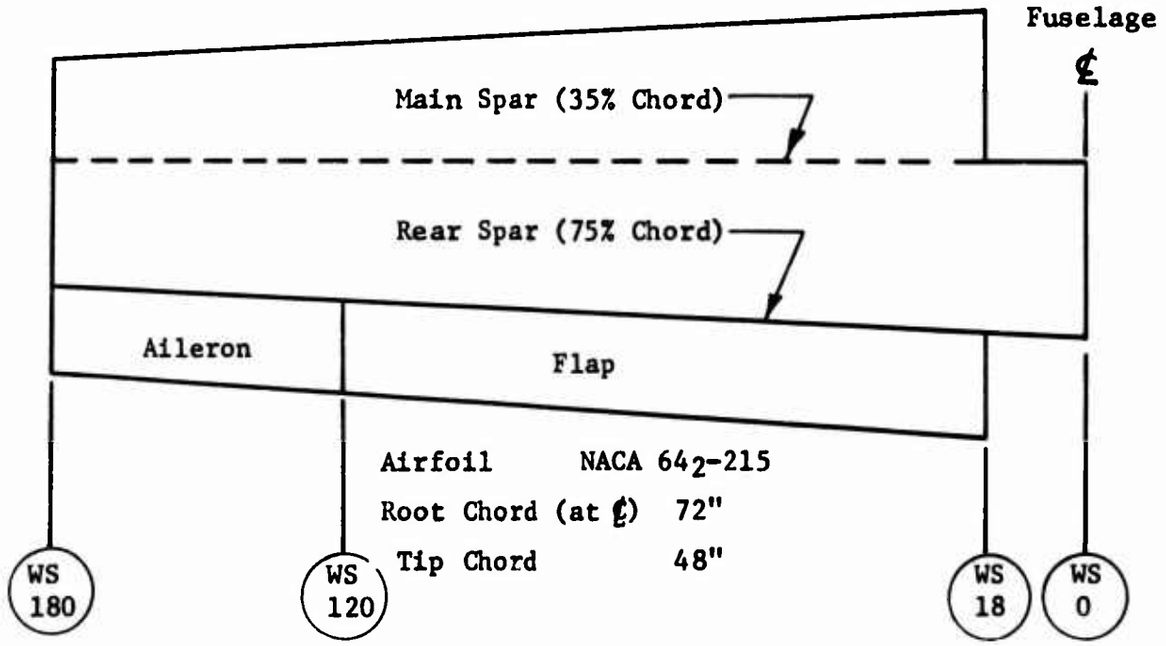

Figure 24. Wing Configuration.

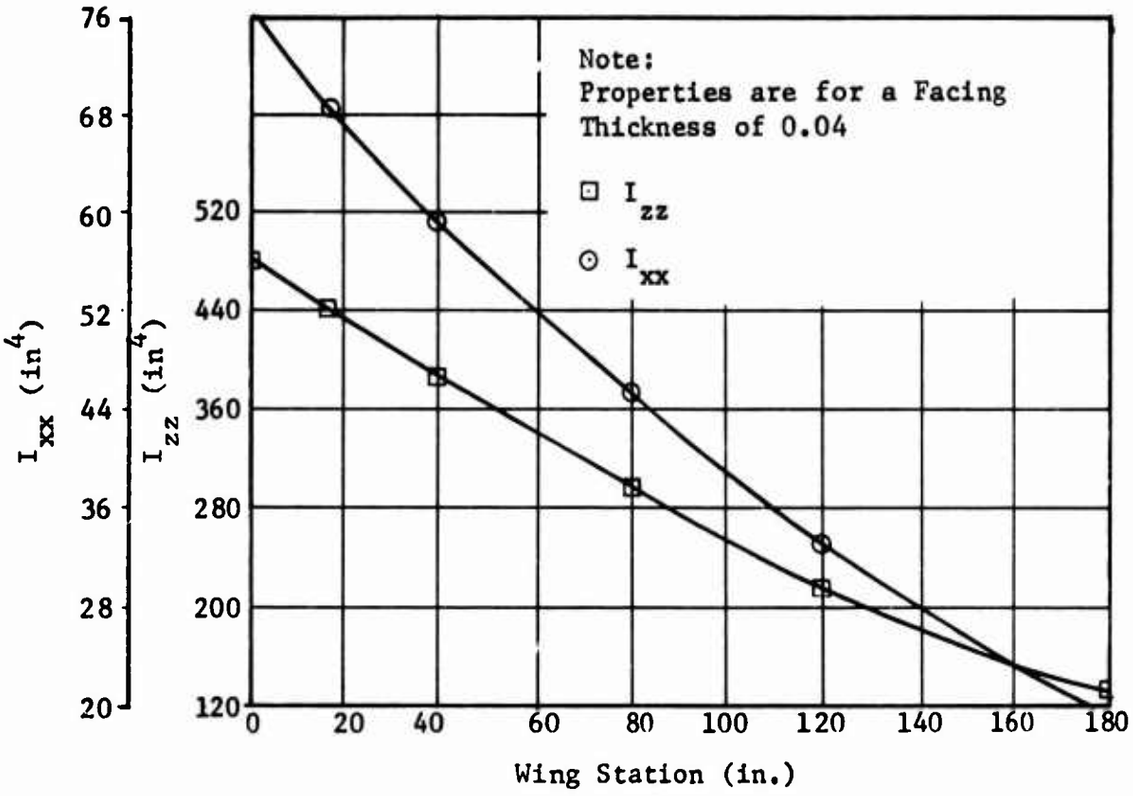

Figure 25. Wing Section Properties I_{xx}, I_{zz}.

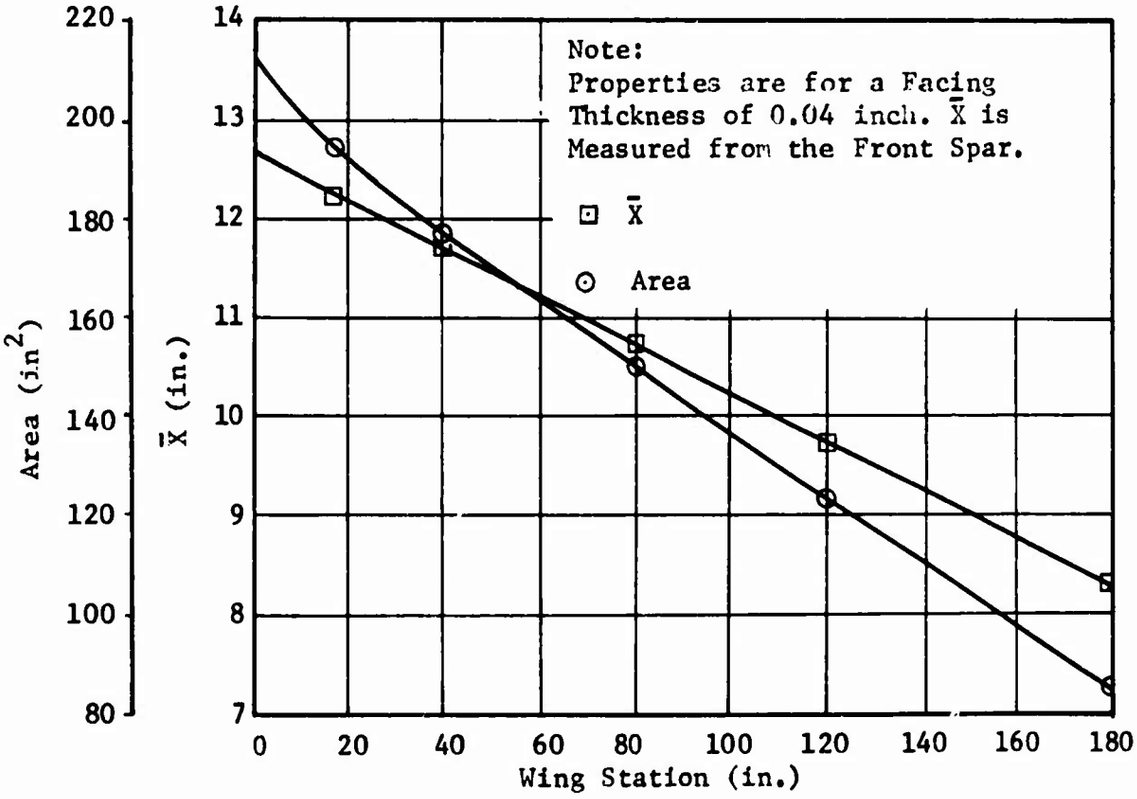

Figure 26. Wing Section Properties - Area, $\bar{X}$.

Using the equations given in Reference 7, the following properties were calculated:

$$E_L = 6.743 \times 10^6 \text{ psi} \qquad \mu_{LT} = .2634$$

$$E_T = 2.152 \times 10^6 \text{ psi} \qquad \mu_{TL} = .0841$$

The average composite properties can now be calculated in any direction of a multilayer composite by using the following equations:

$$E_\alpha = \frac{1}{\frac{\cos \alpha}{E_L} + \frac{\sin \alpha}{E_T}}, \tag{1}$$

$$E_y = \frac{N_L E_L + N_T E_T + N_\alpha E_\alpha}{N_L + N_T + N_\alpha}, \tag{2}$$

$$E_x = \frac{N_T E_L + N_L E_T + N_\alpha E_{90-\alpha}}{N_L + N_T + N_\alpha}, \tag{3}$$

$$\mu_{\alpha L} = \mu_{LT} \frac{E_\alpha}{E_L}, \tag{4}$$

$$\mu_{yx} = \frac{N_L \mu_{LT} + N_T \mu_{TL} + N_\alpha \mu_{\alpha L}}{N_L + N_T + N_\alpha}, \tag{5}$$

$$\mu_{xy} = \mu_{yx} \frac{E_x}{E_y}. \tag{6}$$

The design of the wing section dictated a facing thickness of 0.040 inch or four layers at 0.010 inch per layer. The layers are oriented at 0°, 45°, and 90° to the y axis. With this orientation, the following properties are calculated from equations (1) through (6):

$$E_x = E_y = 3.375 \times 10^6 \text{ psi},$$

$$\mu_{xy} = \mu_{yx} = 0.132.$$

The allowable strength values for the above orientation are taken from HITCO test results of nonwoven oriented laminates. The average values of typical laminates are as follows:

$$F_c = 49{,}000 \text{ psi}, \qquad F_t = 45{,}000 \text{ psi},$$

$$F_s = 32{,}000 \text{ psi}.$$

MARGINS OF SAFETY

A summary of the safety margins and allowables is shown in Table XVII. The margin of safety is calculated by using the following equations:

For Stress Analysis

$$M.S. = \frac{F_{all}}{\sigma} - 1. \tag{7}$$

For Buckling Analysis (see Reference 6, page 1.5.3.5)

$$M.S. = \frac{2}{\frac{N_c}{N_{ccr}} + \sqrt{\left(\frac{N_c}{N_{ccr}}\right)^2 + 4\left[\left(\frac{N_s}{N_{scr}}\right)^2 + \left(\frac{N_b}{N_{bcr}}\right)^2\right]}} - 1. \tag{8}$$

STRESS ANALYSIS

1. Primary Bending Stresses

The spanwise bending stresses are calculated for M_z and M_x from equations (9) and (10):

$$N_y = \pm \frac{M_x c}{I_{xx}} \pm \frac{M_z c}{I_{zz}}, \tag{9}$$

$$\sigma_y = \frac{N_y}{2t_f}. \tag{10}$$

Figure 27 shows the spanwise load (N_y) in pounds per inch at station 18.

2. Shear Stresses

The shear stresses are calculated for the torsion and shear loads (M_y, V_z, V_x) by using equations (11) and (12):

$$\tau = \frac{q}{2t_f}, \tag{11}$$

$$q = \pm \frac{T}{2A} \pm \frac{V_z Q_z}{2I_{xx}} \pm \frac{V_x Q_x}{2I_{zz}}, \tag{12}$$

where

T is the total torsional load with reference to the center of gravity.

$$Q_z = \int z \, dA$$

$$Q_x = \int x \, dA$$

Figure 28 shows the shear flow diagram for station 18.

3. Buckling Analysis

The top flange is in compression and must be analyzed for buckling. The shears and compressive loads causing instability are shown in Figures 27 and 28. The core thickness required to prevent buckling is calculated by rewriting the panel buckling equations shown in Reference 3. Equation (13) is a summary of these equations:

$$t_c = \frac{-B \pm \sqrt{B^2 - 4C}}{2}, \tag{13}$$

where

$$B = 2t_f \left(1 - \frac{F_{ycr}}{K'}\right).$$

$$C = \frac{4t_f^2}{3} - \frac{2F_{ycr}}{R'}.$$

$$F_{ycr} = \frac{N}{2t_f}.$$

$$K' = G_{yz} + G_{xz} \frac{a^2}{b^2}.$$

$$R' = \frac{\pi^2}{2\lambda b^2} \left(E_x \frac{a^2}{b^2} + E_y \frac{b^2}{a^2} + 2A\right).$$

$$A = E_x \mu_{yx} + 2\lambda G_{xy}.$$

$$\lambda = 1 - \mu_{xy}\mu_{yx}.$$

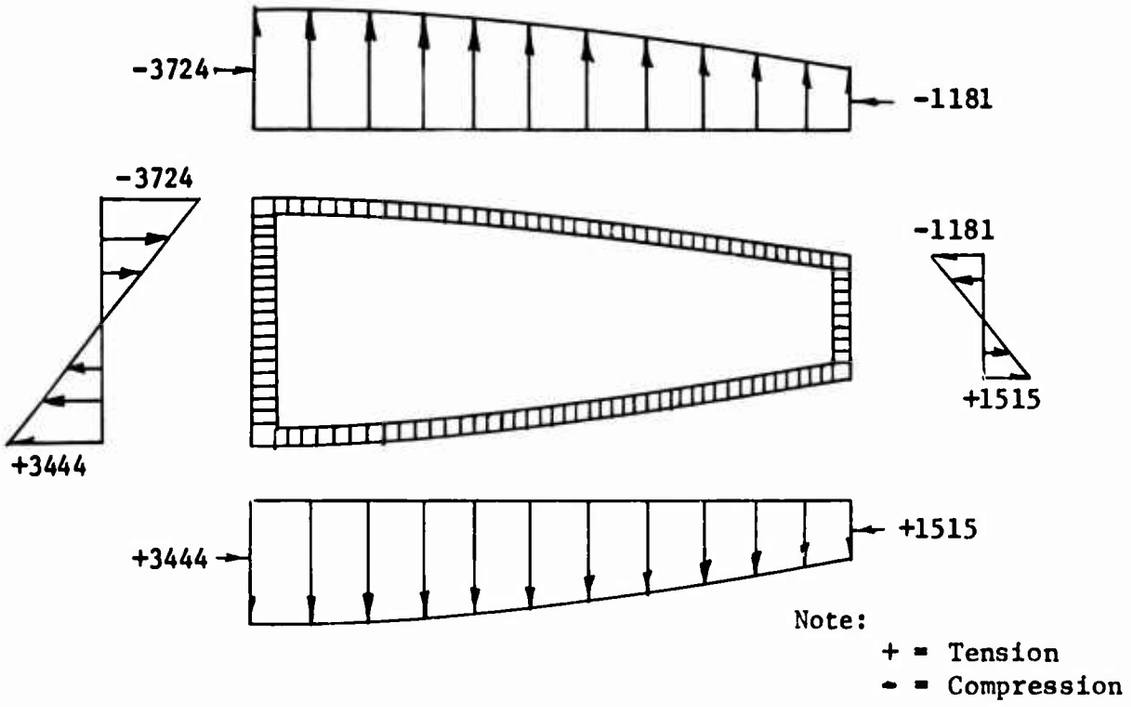

Figure 27. Spanwise Load in Pounds/Inch at Station 18.

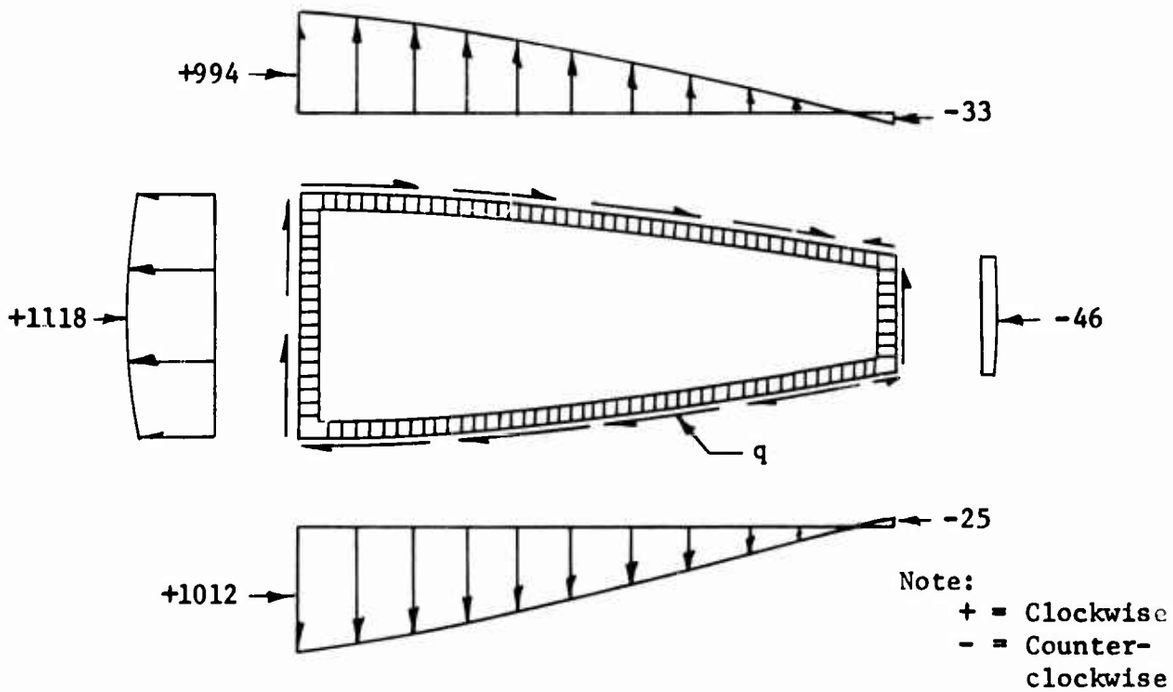

Figure 28. Shear Load in Pounds/Inch at Station 18.

N is the average compressive load on the panel, $\frac{N_{max} + N_{min}}{2}$

$\frac{a}{b} = 1$ for all buckling analysis gives the lowest critical load.

This analysis gives a core thickness (t_c) of 0.90 inch. The analysis, however, does not include the shear loads on the panel nor the uneven compressive load which can be added as a bending load on the panel. To include these effects, the thickness of the core was increased to 0.92 inch and the panel was checked using References 1 and 2. This analysis gives the following critical loads:

$$N_{scr} = 5444 \text{ pounds/inch},$$

$$N_{bcr} = 15{,}076 \text{ pounds/inch},$$

$$N_{ccr} = 2781 \text{ pounds/inch}.$$

These critical loads are independent of each other and are added together by the interaction equation to determine if the panel is critical in buckling. This is done as shown in equation (8) where the calculated loads are as shown below:

$$N_s = 994 \text{ pounds/inch},$$

$$N_b = 1271 \text{ pounds/inch},$$

$$N_c = 2452 \text{ pounds/inch}.$$

4. Chordwise Bending Stresses

The chordwise stresses are determined from a secondary load analysis. The tensile and compressive forces (N_y) in the beam flanges cause a beam curvature of radius R as shown in Figure 29.

The equilibrium forces are then normal to the flange surfaces as shown by p_s in Figure 29. These normal pressures are beamed across the flange to the spars which act as compression members. This normal pressure is then found from equation (14):

$$p_s = \frac{N_y}{R} . \tag{14}$$

And from the moment-radius of curvature relationship,

$$\frac{1}{R} = \frac{E_y I}{M_x \left(1 - \mu_{yx}\mu_{xy}\right)} . \tag{15}$$

The final equation for determining this normal pressure is then found by substituting equation (15) into equation (14):

$$p_s = \frac{N_y M_x \left(1 - \mu_{xy}\mu_{yx}\right)}{E_y I} . \tag{16}$$

The total pressure (p_t) acting on the beam is found by adding the secondary normal pressure to the air pressure:

$$p_t = p_s + p_a . \tag{17}$$

A pressure distribution curve at station 18 is shown in Figure 30.

The chordwise stresses are found by substituting the moments and shears (Appendix II) into the following equations:

$$\sigma_x = \pm \frac{Mc}{I} \text{ (maximum flange stress)}, \tag{18}$$

$$\sigma_x = \pm \frac{Mc}{I} + \frac{P}{2t_f} \text{ (maximum spar stress)}. \tag{19}$$

A summary of all the stresses is shown in Table XVIII, page 65.

DEFLECTION ANALYSIS

1. Spanwise Deflection

The spanwise deflection is calculated by using the conjugate beam method of analysis. The M/EI diagram for the airfoil is shown in Figure 31 with the actual loading and the loading assumed for this analysis. This loading is then placed on the conjugate beam as shown in Figure 32, and M/EI becomes the loading for calculating the deflection. The deflection at any point can be calculated by applying equations (20) and (21):

$$(\delta)_{x=a,b} = \frac{wx^2}{2} - \frac{wx^3}{6L_{ab}} , \tag{20}$$

$$(\delta)_{x=b,c} = \frac{wL_{ab}}{2}\left(x - \frac{L_{ab}}{3}\right) , \tag{21}$$

where

$$w = \frac{M}{EI} .$$

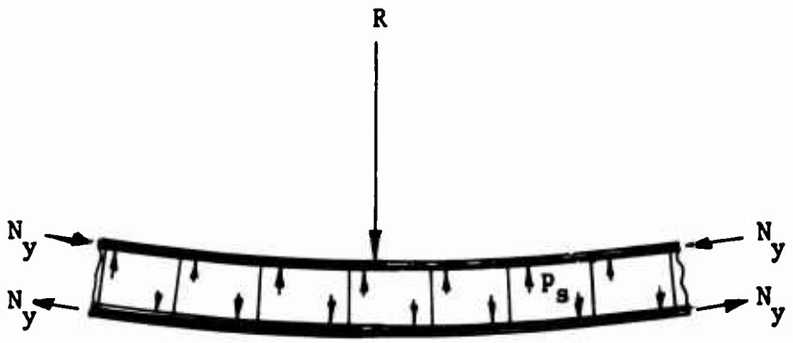

Figure 29. Secondary Load Diagram.

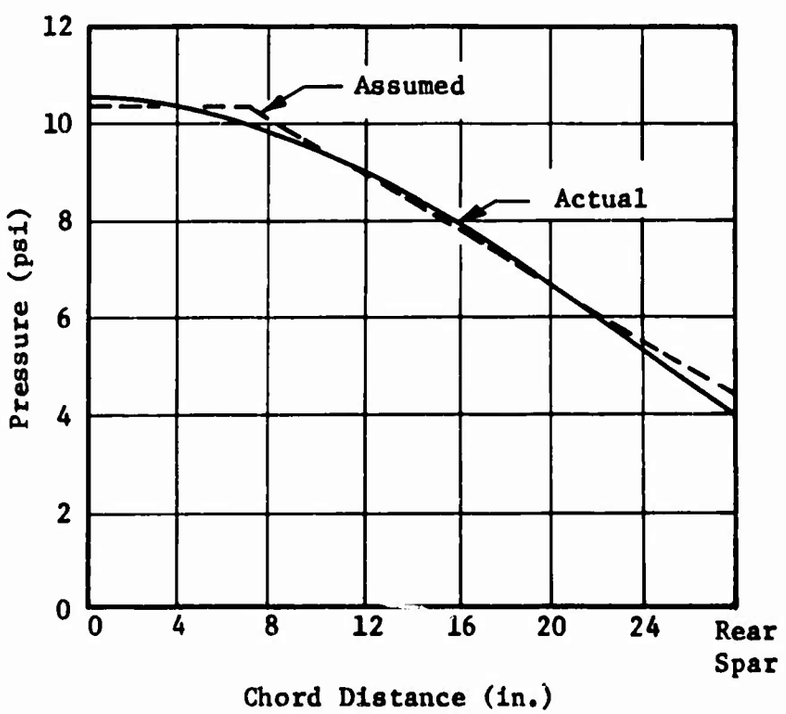

Figure 30. Pressure Distribution at Station 18.

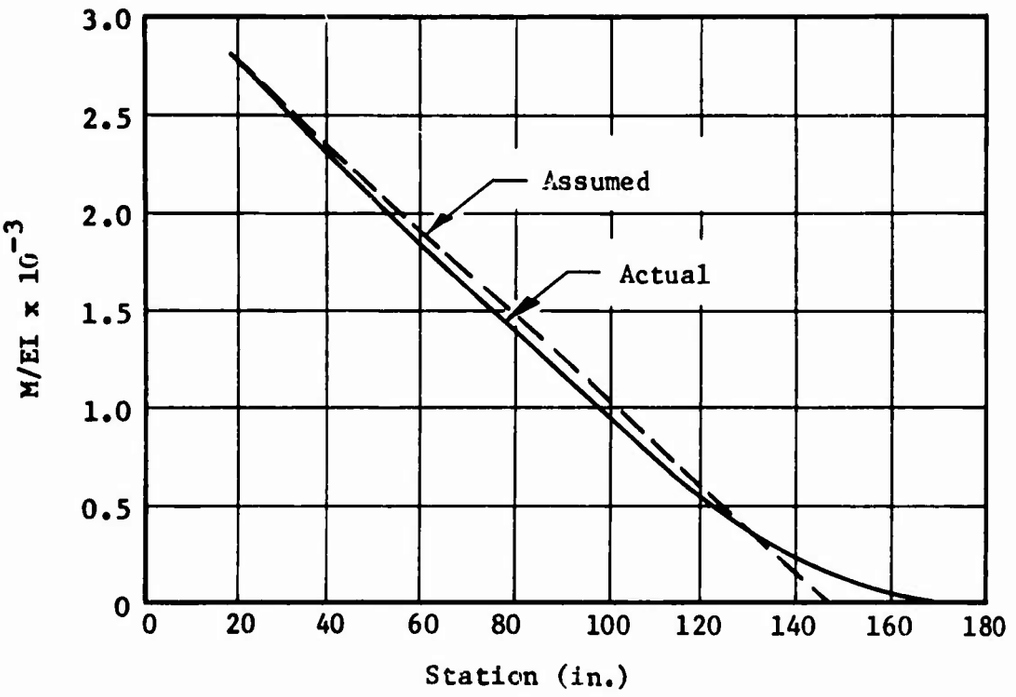

Figure 31. Wing M/EI Diagram.

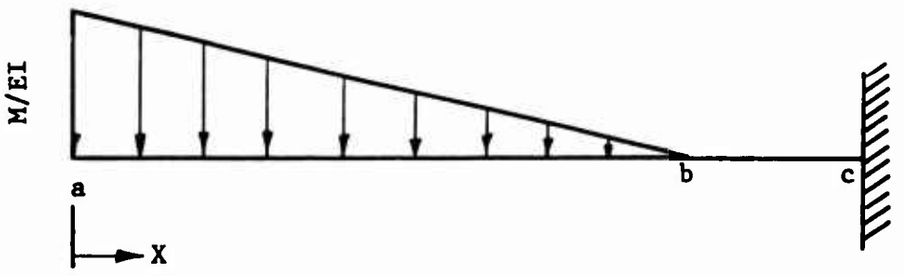

Figure 32. M/EI Conjugate Beam Diagram.

2. Torsional Rotation of Airfoil Section

The rotation is calculated by using equation (22):

$$\phi = \sum \frac{TL}{GJ} , \tag{22}$$

where

$$J = \frac{4A^2 t^*}{S} .$$

A = Area.

G = Shear modulus of the faces.

L = Incremental length.

T = Torsional moment.

S = Periphery length.

3. Chordwise Deflection

The assumed loading condition shown in Figure 30 is used to calculate the chordwise deflection. The edge moments M and M' are those calculated in Appendix II. Equation (23) gives the midbay deflections at operating loads:

$$\delta_c = \frac{5WL_{bd}^4}{384E_yI} - \frac{(M + M')L_{bd}^2}{16E_yI} + .00652 \frac{W_1 L_{bd}^5}{L_{bc}E_yI}$$

$$- \frac{W_1}{E_yI}\left(\frac{L_{bd}}{L_{bc}} - 1\right)\left(.00781\ L_{cd}^2\ L_{bd}^2 - .00416\ L_{cd}^4\right) \tag{23}$$

where W and W_1 are the loadings as shown in Figure 33, Appendix II.

A summary of all deflections and rotations at limit load is shown in Table XVIII.

*Reference 5, pages 486-488.

TABLE XVII
SAFETY MARGIN SUMMARY

	Allowable	Applied	Safety Margin
Spanwise Compressive Stress (psi) (Flange)	49,000	46,550	+ .053
Spanwise Tensile Stress (psi) (Flange)	45,000	43,050	+ .045
Chordwise Tensile Stress (psi) (Flange)	45,000	11,700	+2.84
Chordwise Compressive Stress (psi) (Spar)	49,000	12,900	+2.80
Shear Stress (psi) (Flange)	32,000	12,650	+1.53
Shear Stress (psi) (Spar)	32,000	13,980	+1.29
Buckling Load (pounds/inch) (Flange)	N_{scr} = 5444 N^{b}_{scr} = 15,076 N^{b}_{ccr} = 2781	N_s = 994 N^{s}_{b} = 1271 N^{b}_{c} = 2452	+ .003
Face Wrinkling (psi)	64,000	46,550	+ .37
Buckling Load (pounds/inch) (Front Spar)	N_{scr} = 48,002 N^{s}_{bcr} = 128,377 N^{b}_{ccr} = 10,605	N_s = 1118 N^{s}_{b} = 3584 N^{b}_{c} = 0	+High

TABLE XVIII
STRESS AND DEFLECTION ANALYSIS SUMMARY

Station	Spanwise Stress[1]	Chordwise Stress		Shear Stress		δ_y[4] (inches)	δ_y[5] (inches)	θ[6] (degrees)
		Flange	Spar[2]	Flange	Spar[3]			
18	-46,550 +43,050	±11,700	-12,900	12,650	13,980	0	.210	0
40	-36,220 +33,470	± 7,400	- 8,200	10,660	11,775	.4268	.113	1.007
60	-28,380 +26,250	± 4,500	- 5,000	10,000	11,120	1.4703	.062	1.894
80	-21,000 +19,540	± 2,400	- 2,700	8,000	8,850	3.0183	.033	2.665
100	-14,120 +13,625	± 1,100	- 1,300	6,130	6,750	4.9548	.014	3.296
120	- 7,130 + 6,730	± 500	- 600	4,410	4,890	7.1638	.005	3.789
140	- 2,250 + 2,000	± 200	- 250	2,900	3,160	9.5294	.0015	4.142
160	- 500 + 450	± 50	- 70	1,450	1,570	11.9409	.0002	4.354
180	0	0	0	0	0	14.3532	0	4.427

Notes: All stresses are in psi at ultimate loads.
1. Compression (-) on top flange and tension (+) on lower flange.
2. Maximum stress in rear spar.
3. Maximum shear stress in front spar.
4. Spanwise deflection at operating loads.
5. Chordwise deflection at midbay at operating loads.
6. Spanwise rotation at operating loads.

APPENDIX II
DERIVATION OF SECONDARY BENDING EQUATIONS

The chordwise bending stresses are caused by beaming the normal loads, due to air pressure (p_a) and pressures caused by secondary loading (p_s), shown on page 60, to the box beam spars. In this analysis, it is assumed that the loading is symmetrical, and a unit width of the box beam is treated as a frame. The method of least work is used to evaluate the bending moments.

Figure 33 shows the frame free body diagram.

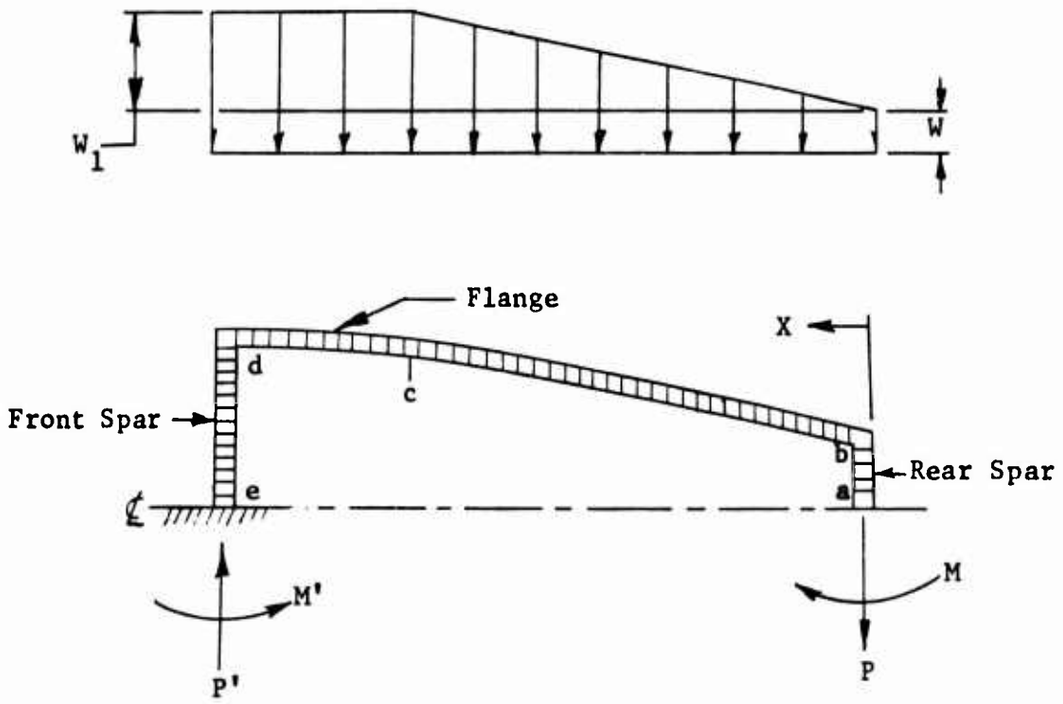

Figure 33. Free Body Diagram for Frame Analysis.

The vertical deflection at "a" due to the loading shown in Figure 33 is

$$\delta_v = \int_b^d \frac{mMdx}{E_y I}, \tag{24}$$

where

$$M = \int_b^d \frac{Wx^2}{2} + \int_b^c \frac{W_1 x^3}{6L_{bc}} + \int_c^d \frac{W_1 L_{bc}^2}{6} + \frac{W_1 L_{bc}}{2}\left(x - L_{bc}\right) + \frac{W_1\left(x-L_{bc}\right)^2}{2}, \tag{25}$$

$m = x$.

Making the above substitutions and integrating equation (24) results in the first equation:

$$\delta_v = \frac{1}{E_y I}\left[W\left(\frac{L_{bd}^4}{8} + \frac{L_{bd}^3 L_{de}}{2}\right) + W_1\left(-\frac{L_{bc}^4}{120} + \frac{L_{bc}^2 L_{bd}^2}{12}\right.\right.$$

$$\left.\left. - \frac{L_{bc} L_{bd}^3}{6} + \frac{L_{bd}^4}{8} + \frac{L_{bc} L_{bd}^2 L_{de}}{2} - \frac{L_{bc}^2 L_{bd} L_{de}}{3} + \frac{L_{cd}^2 L_{bd} L_{de}}{2}\right)\right]. \qquad (26)$$

The rotational deflection at "a" due to the loading shown in Figure 33 is

$$\delta_\theta = \int_b^d \frac{mMdx}{E_y I}, \qquad (27)$$

where M is the same as equation (25):

$$m = 1.0.$$

Substituting these into equation (27) and integrating results in the second equation:

$$\delta_\theta = \frac{1}{E_y I}\left[W\left(\frac{L_{bd}^3}{6} + \frac{L_{bd}^2 L_{de}}{2}\right) + W_1\left(-\frac{L_{bc}^3}{24} + \frac{L_{bd}^3}{6}\right.\right.$$

$$\left.\left. - \frac{L_{bd}^2 L_{bc}}{4} + \frac{L_{bc}^2 L_{bd}}{6} + \frac{L_{bc} L_{bd} L_{de}}{2} - \frac{L_{bc}^2 L_{de}}{3} + \frac{L_{cd}^2 L_{de}}{2}\right)\right]. \qquad (28)$$

The vertical deflection at "a" due to a shear load (P) at "a" equal to unity is

$$\delta_{vp} = \frac{1}{E_y I}\int_b^e \frac{mMdx}{EI}, \qquad (29)$$

where

$$M = \int_b^d x + \int_d^e L_{bd},$$

$$m = \int_b^d x + \int_d^e L_{bd}.$$

Substituting and integrating equation (29) gives the third equation:

$$\delta_{vp} = \frac{1}{E_y I}\left(\frac{L_{bd}^3}{3} + L_{bd}^2 L_{de}\right). \tag{30}$$

The rotational deflection at "a" due to a shear load (P) at "a" equal to unity is

$$\delta_{\theta p} = \frac{1}{E_y I}\int_a^e \frac{mMdx}{EI}, \tag{31}$$

where

$$M = \int_b^d x + \int_d^e L_{bd},$$

$$m = 1.0.$$

Substituting and integrating gives

$$\delta_{\theta p} = \frac{1}{E_y I}\left(\frac{L_{bd}^2}{2} + L_{bd}L_{de}\right). \tag{32}$$

The vertical deflection at "a" due to a unit clockwise moment (M) at "a" is

$$\delta_{vm} = \int_a^e \frac{Mmdx}{E_y I}, \tag{33}$$

where

$$M = 1.0$$

$$m = \int_a^b 0 + \int_b^d x + \int_d^e L_{bd}$$

Substituting and integrating gives

$$\delta_{vm} = \frac{1}{E_y I}\left(\frac{L_{bd}^2}{2} + L_{bd}L_{de}\right). \tag{34}$$

The rotational deflection at "a" due to a unit clockwise moment (M) at "a" is

$$\delta_{\theta m} = \int_a^e \frac{Mmdx}{E_y I} , \tag{35}$$

where

$M = 1.0,$

$m = 1.0.$

Substituting and integrating gives

$$\delta_{\theta m} = \frac{1}{E_y I} \left(L_{bd} + L_{de} + L_{ab} \right) . \tag{36}$$

To satisfy equilibrium of the free body shown in Figure 33, with no rotation nor deflection at "a", two equations can be written with the two unknowns M and P:

$$\delta_v + P\,\delta_{vp} + M\,\delta_{vm} = 0, \tag{37}$$

$$\delta_\theta + P\,\delta_{\theta p} + M\,\delta_{\theta m} = 0. \tag{38}$$

M and P can be found by substituting equations (26), (28), (30), (32), (34), and (36) into equations (37) and (38) and solving simultaneously.

With M and P known, the moment (M') and shear (P') forces at "e" can now be found from the following conditions:

$$\Sigma F_v = 0, \tag{39}$$

$$\Sigma M_e = 0. \tag{40}$$

Solving equations (39) and (40) gives

$$M' = M + \frac{WL_{bd}^2}{2} + \frac{W_1 L_{cd}^2}{2} + \frac{W_1 L_{bc}}{2} \left(L_{cd} + \frac{L_{bc}}{3} \right) + PL_{bd} , \tag{41}$$

$$P' = WL_{bd} + W_1 L_{cd} + \frac{W_1 L_{bc}}{2} + P. \tag{42}$$

The following values were found at station 18 using equations (37), (38), (41), and (42):

$M = 487$ inch-pounds/inch (clockwise),

$M' = 382$ inch-pounds/inch (counterclockwise),

$P = 101$ pounds/inch (upward),

$P' = 124$ pounds/inch (upward).

APPENDIX III
FABRICATION PROCEDURES

BOX BEAM NO. 1

Step 1. Mold release mandrel and caul sheets with RAM 225 mold release.

Step 2. Hand lay-up inside spar faces on mandrel. (See spar fabrication procedure.)

Step 3. Hand lay-up inside flange faces on mandrel with material 1 in the following sequence:

Layer 1 - Longitudinals (spanwise layer)
Layer 2 - 1st 45 degrees
Layer 3 - 2nd 45 degrees (oriented 90 degrees from 1st 45-degree layer)
Layer 4 - Hoops (chordwise layer)

Step 4. Place one layer of Metlbond 400 adhesive film over inside face and spars.

Step 5. Place prefabricated syntactic foam corners over adhesive film.

Step 6. Cut and place .460-inch thick HRP 3/16-GF 11-4.0 honeycomb core over the adhesive film between foam corners (ribbon direction to be spanwise direction).

Step 7. Place one layer of adhesive film over the honeycomb and syntactic foam corners.

Step 8. Place prefabricated outside spar face over the spar section.

Step 9. Hand lay-up outside flange faces with material 1 in the same sequence as Step 3.

Step 10. Place 0.016-inch-thick aluminum caul sheet over flanges and tape in position.

Step 11. Hand wrap beam with Tedlar tape and heavy cotton bleeder cloth.

Step 12. Bag with a Tedlar bag.

Step 13. Cure at 50-psi autoclave pressure and cure cycle 2. Maintain vacuum on part throughout cure cycle.

Step 14. Remove vacuum bag, overwrap and caul sheet from beam, take out mandrel, and trim the beam.

BOX BEAMS NO. 2 THROUGH 6

Step 1. Mold release mandrel, caul sheets, and threaded rods with RAM 225 mold release.

Step 2. Place prefabricated inside spar faces on mandrel.

Step 3. Attach side plates to mandrel and set up in winding machine to wind the longitudinal fibers.

Step 4. Wind longitudinal layer with material 2. Set lead at .069 inch for an end count of 290 ends/inch.

Step 5. Install the first set of threaded rods and 45-degree end arms to the mandrel and wind the first layer of 45-degree fibers with material 2 at the same lead and end count as in Step 4.

Step 6. Add the second set of threaded rods to the mandrel and reverse the 45-degree end arms. Wind the second layer of 45-degree fibers with material 2 at the same lead and end count as in Step 4.

Step 7. Apply extra resin to the 45-degree fibers as necessary.

Step 8. Remove the end arms and set the mandrel up in the winding machine for winding the hoop (chordwise) fibers.

Step 9. Wind the hoop fibers with material 2 at the same lead and end count as in Step 4.

Step 10. Place 1 ply of preimpregnated 120 cloth/E787 over the hoop fibers for a tear ply.

Step 11. Place the caul sheets (0.016-inch-thick aluminum) over the flange sections.

Step 12. Place a heavy cotton bleeder material over the part and bag with a Teflon bag.

Step 13. Cure inside face per cure cycle 2.

Step 14. Remove bag and caul sheets and trim and clean inner face.

Step 15. Remove tear ply.

Step 16. Sand flanges lightly for a good bond to the honeycomb core.

Step 17. Place 1 ply of Metlbond 329 adhesive film over the inside face (spar and flange).

Step 18. Place 1 ply of adhesive on the inside surfaces of the prefabricated outer spar faces.

Step 19. Place prefabricated syntactic foam corners into the outer spar corners over the adhesive.

Step 20. Cut and place honeycomb core between the corner sections inside the outer spar faces.

Step 21. Place outer spar faces over the inner spar faces which are covered with adhesive film.

Step 22. Cut and place honeycomb core over the flange sections.

Step 23. Place heavy cotton bleeder cloth over the part and bag with a Teflon bag and cure with 5-10-psi vacuum bag pressure at cure cycle 1.

Step 24. Remove bag.

Step 25. Repeat Steps 3 through 9.

Step 26. Repeat Steps 11 and 12.

Step 27. Cure completed part per cure cycle 2.

Step 28. Remove the bag, bleeder cloth, and caul sheets.

Step 29. Remove the part from the mandrel.

Step 30. Trim and clean the part.

A. Box Beam No. 2

Box beam No. 2 is fabricated as shown above with the following changes:

1. Eliminate Step 7.
2. Eliminate Step 10.
3. Eliminate Step 15.

B. Box Beam No. 3

Box beam No. 3 is fabricated as shown above with the following changes:

1. Eliminate Step 7.
2. Step 9 was revised to include "begin hoop wrap at station 0 (the large end) and stop at station 45 (midspan of the mandrel)."
3. Eliminate Step 10.
4. Eliminate Step 15.

C. Box Beam No. 4

Box beam No. 4 is fabricated as shown above with the following changes:

1. Eliminate Step 7.
2. Revise Step 9 to include "begin hoop wrap at station 0 (the large end) and stop at station 45 (midspan of the mandrel)."
3. Eliminate Step 16.
4. Steps 4, 5, 6, and 9 change from material 2 to material 3.

D. Box Beams No. 5 and No. 6

Box beams No. 5 and 6 are fabricated as shown above with the following change:

Eliminate Step 16.

SPAR FABRICATION

Step 1. Mold release spar molds with RAM 225 mold release.

Step 2. Prepare material 1 for the spars.

Step 3. Hand lay-up 4 plies of the prepared material on the spar molds in the following sequence:

Layer 1 - Longitudinals (spanwise layer)
Layer 2 - 1st 45-degree layer
Layer 3 - 2nd 45-degree layer oriented 90 degrees to the 1st 45-degree layer
Layer 4 - Hoops (chordwise layer)

Step 4. Place 1 ply of preimpregnated 120 cloth/E787 over the inside faces.

Step 5. Place caul sheets over the 120 cloth on the inside faces and over the hoop layer of the outside faces.

Step 6. Bag with a Teflon bag.

Step 7. Cure at 50-psi autoclave pressure per cure cycle 1.

Step 8. Remove bag, caul sheets, and 120 cloth as required and trim spar faces.

MATERIALS AND CURE CYCLES

Material 1 - E-HTS/XP-251 12-inch-wide unidirectional tape with an end count of 200 ends/inch.

Material 2 - E-HTS/E787 20 end roving.

Material 3 - S-994/E787 20 end roving.

Cure Cycle 1 - Cure 325°F/3 hours.

Cure Cycle 2 - Cure 275°F/3 hours
Postcure 325°F/4 hours

Metlbond 400 adhesive film

Metlbond 329 adhesive film

HRP 3/16-GF 11-4.0 reinforced plastic honeycomb.

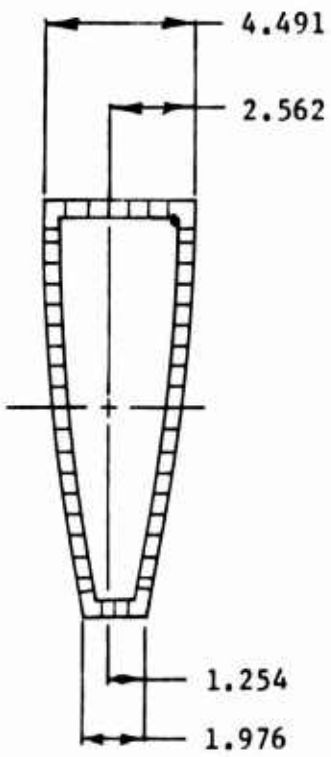

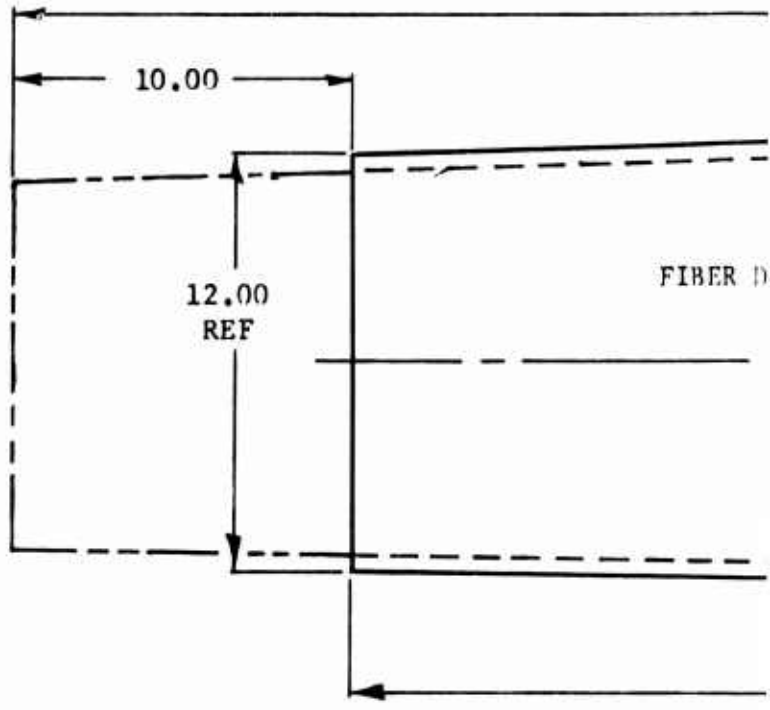

FLANGE SCHEDULE

ASSY NO.	LAYER 1			LAYER 2			LAYER 3			LAYER 4			PART CURE
	α	FAB	MATL	α	FAB	MATL	α	FAB	MATL	α	FAB	MATL	
-1	0°	2	5	45°	2	5	135°	2	5	90°	2	5	8
-2	0°	3	4	45°	3	4	135°	3	4	90°	3	4	14
-3	0°	3	4	45°	3	4	135°	3	4	90°	12	4	14
-4	0°	3	11	45°	3	11	135°	3	11	90°	12	11	14
-5	0°	3	4	45°	3	4	135°	3	4	90°	3	4	14
-6	0°	3	4	45°	3	4	135°	3	4	90°	3	4	14

FIGURE 34. BOX BEAM 1/2 SCALE MODEL

APPENDIX IV

DRAWING SKRD 0607, BOX BEAM 1/2 SCALE MODEL

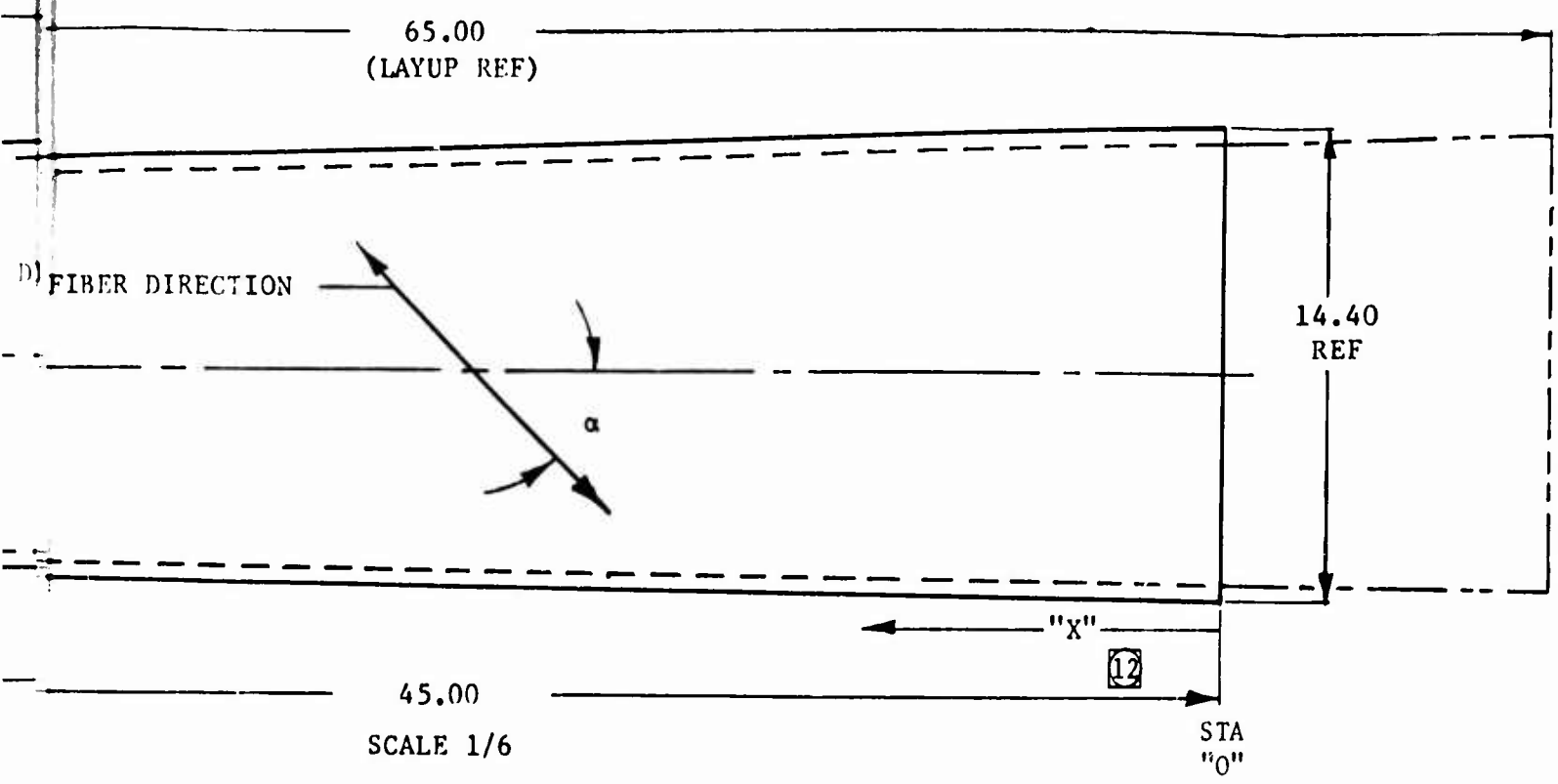

SPAR SCHEDULE

LAYER 1			LAYER 2			LAYER 3			LAYER 4		
α	FAB	MATL	α	FAB	MATL	α	FAB	MATL	α	FAB	MATL
0°	(2)	(5)	45°	(2)	(5)	135°	(2)	(5)	90°	(2)	(5)

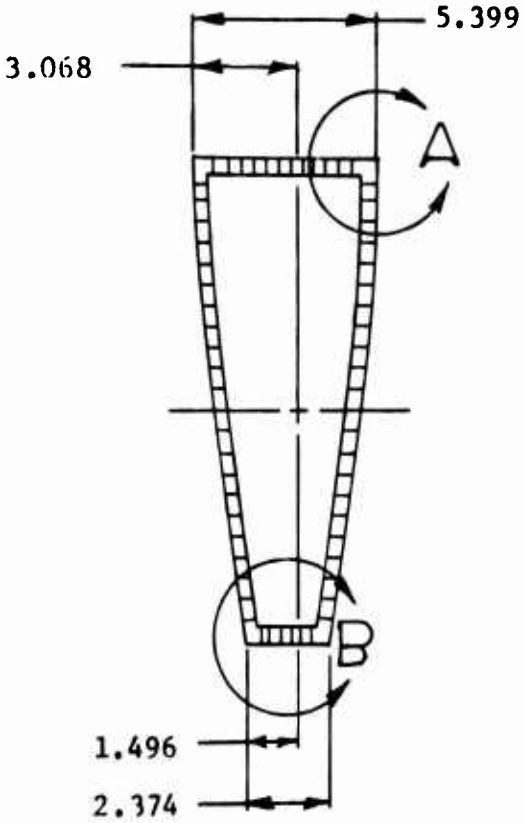

LAYER 4		
α	FAB	MATL
90°	2	5

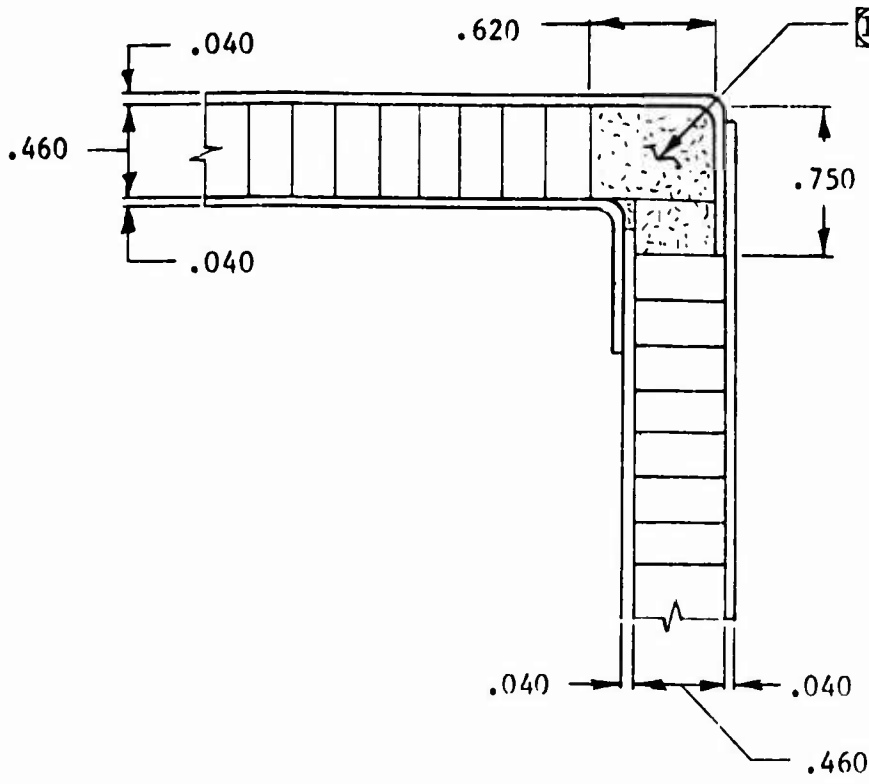

DETAIL A
FULL SCALE
TYP 2 FWD CORNERS

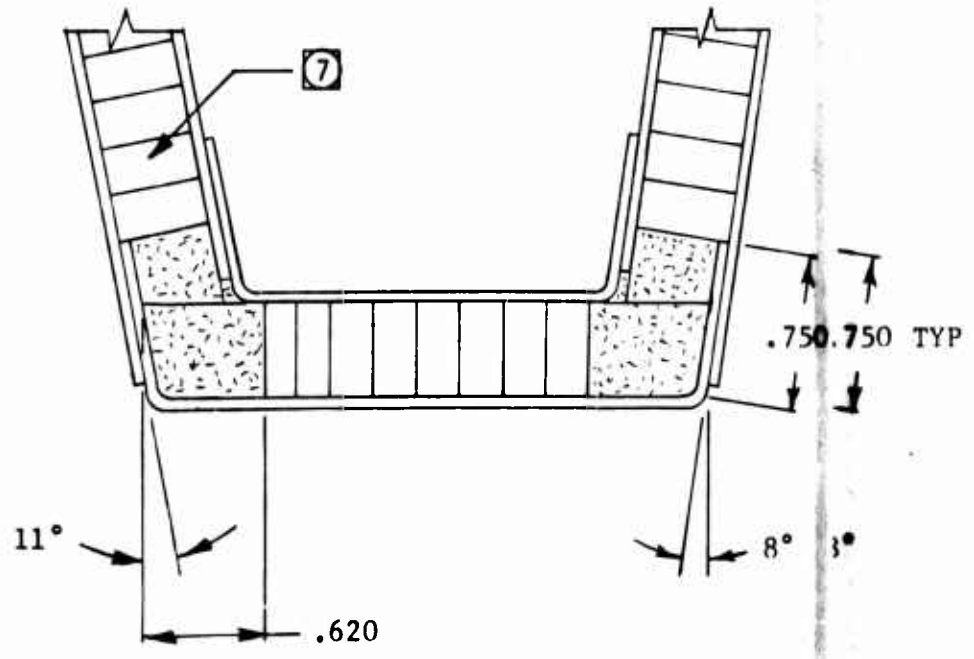

DETAIL B
FULL SCALE

LL.
RS

NOTES

1. LAYER NO. 1 IS ON THE IML OF BOTH INNER AND OUTER FACES AS FABRICATED.

(2). HAND LAYUP.

(3). MACHINE FILAMENT WIND, TENSION 3 LBS/20 END ROVING.

(4). MATL: 20 END "E"-HTS ROVING PREIMPREGNATED WITH E/787 RESIN. 23 ± 3% RESIN CONTENT. U.S. POLYMERIC OR EQUIV.

(5). MATL: UNIDIRECTIONAL "E" GLASS FILAMENT TAPE, PREIMPREGNATED WITH XP-251 RESIN, 23 ± 3% RESIN CONTENT, 196 ENDS/INCH. 3M CO. OR EQUIV.

(6). MATL: GLASS FABRIC 143 STYLE PREIMPREGNATED WITH E/787 RESIN, 23 ± 3% RESIN CONTENT. U.S. POLYMERIC OR EQUIV.

(7). CORE: HP 3/16-4 LB/FT^3 HONEYCOMB. HEXCELL OR EQUIV.

(8). AUTOCLAVE CURE AT 50 PSI, 2 HOURS @ 225°F, 3 HOURS @ 325°F. LEAVE UNDER PRESSURE UNTIL COOLED TO 100°F.

(9). AF 110-B ADHESIVE FILM. 3M CO. OR EQUIV.

(10). MATL: SYNTACTIC FOAM, 44 LB/FT^3. 3M CO. OR EQUIV.

(11). MATL: 20 END S-994 ROVING PREIMPREGNATED WITH E/787 RESIN, 23 ± 3% RESIN CONTENT. U.S. POLYMERIC OR EQUIV.

(12). MACHINE FILAMENT WIND, TENSION 3 LBS/20 END ROVING. WIND ONLY TO X = 22.5.

13. APPLY 1 PLY (9) BETWEEN CORE AND SKIN, TYP INNER AND OUTER SKIN.

(14). VACUUM CURE AT 5 TO 10 LBS, 2 HOURS @ 225°F, 3 HOURS @ 325°F. LEAVE UNDER VACUUM UNTIL COOLED TO 100°F.

P

D

Unclassified

Security Classification

DOCUMENT CONTROL DATA - R&D

(Security classification of title, body of abstract and indexing annotation must be entered when the overall report is classified)

1. ORIGINATING ACTIVITY *(Corporate author)*

HITCO
Gardena, California

2a. REPORT SECURITY CLASSIFICATION

2b GROUP

3. REPORT TITLE

Research in Fabrication Techniques for Fiber Glass Reinforced Primary Aircraft Structures

4. DESCRIPTIVE NOTES *(Type of report and inclusive dates)*

5. AUTHOR(S) *(Last name, first name, initial)*

Daines, Jay V.

6. REPORT DATE	7a. TOTAL NO. OF PAGES	7b. NO. OF REFS
October 1966	90	7

8a. CONTRACT OR GRANT NO.

DA 44-177-AMC-326(T)

b. PROJECT NO.
Task
1P121401A14176

c.

d.

9a. ORIGINATOR'S REPORT NUMBER(S)

USAAVLABS Technical Report 66-76

9b. OTHER REPORT NO(S) *(Any other numbers that may be assigned this report)*

10. AVAILABILITY/LIMITATION NOTICES

Distribution of this document is unlimited.

11. SUPPLEMENTARY NOTES

12. SPONSORING MILITARY ACTIVITY

US Army Aviation Materiel Laboratories
Fort Eustis, Virginia

13. ABSTRACT

This report covers the design, fabrication, and testing of glass reinforced plastic (GRP) 1/2 scale models of a main torsion box assembly incorporating an NACA 642-215 airfoil. The structure was designed as a sandwich wall box beam, with nonwoven oriented (NWO) GRP faces and a GRP honeycomb core.

Fabrication techniques for filament winding a double tapered box beam were investigated and a technique was developed which made it possible to filament wind the 45° fibers as well as the hoop and axial oriented fibers. Unidirectional tape, 12 inches wide, made from E-HTS glass filaments and 20 end roving with both E-HTS and S-HTS glass filaments, preimpregnated with an epoxy resin system were utilized in the fabrication of the facings.

Both the hand layup and filament winding techniques of fabricating primary aircraft structures were found to be practical and within the current state of the art.

DD FORM 1 JAN 64 1473

Unclassified

Security Classification

Unclassified

Security Classification

14. KEY WORDS	LINK A		LINK B		LINK C	
	ROLE	WT	ROLE	WT	ROLE	WT
Filament Winding Techniques Glass Reinforced Plastics Aircraft Structural Fabrication						

INSTRUCTIONS

1. ORIGINATING ACTIVITY: Enter the name and address of the contractor, subcontractor, grantee, Department of Defense activity or other organization *(corporate author)* issuing the report.

2a. REPORT SECURITY CLASSIFICATION: Enter the overall security classification of the report. Indicate whether "Restricted Data" is included. Marking is to be in accordance with appropriate security regulations.

2b. GROUP: Automatic downgrading is specified in DoD Directive 5200.10 and Armed Forces Industrial Manual. Enter the group number. Also, when applicable, show that optional markings have been used for Group 3 and Group 4 as authorized.

3. REPORT TITLE: Enter the complete report title in all capital letters. Titles in all cases should be unclassified. If a meaningful title cannot be selected without classification, show title classification in all capitals in parenthesis immediately following the title.

4. DESCRIPTIVE NOTES: If appropriate, enter the type of report, e.g., interim, progress, summary, annual, or final. Give the inclusive dates when a specific reporting period is covered.

5. AUTHOR(S): Enter the name(s) of author(s) as shown on or in the report. Enter last name, first name, middle initial. If military, show rank and branch of service. The name of the principal author is an absolute minimum requirement.

6. REPORT DATE: Enter the date of the report as day, month, year; or month, year. If more than one date appears on the report, use date of publication.

7a. TOTAL NUMBER OF PAGES: The total page count should follow normal pagination procedures, i.e., enter the number of pages containing information.

7b. NUMBER OF REFERENCES: Enter the total number of references cited in the report.

8a. CONTRACT OR GRANT NUMBER: If appropriate, enter the applicable number of the contract or grant under which the report was written.

8b, 8c, & 8d. PROJECT NUMBER: Enter the appropriate military department identification, such as project number, subproject number, system numbers, task number, etc.

9a. ORIGINATOR'S REPORT NUMBER(S): Enter the official report number by which the document will be identified and controlled by the originating activity. This number must be unique to this report.

9b. OTHER REPORT NUMBER(S): If the report has been assigned any other report numbers *(either by the originator or by the sponsor)*, also enter this number(s).

10. AVAILABILITY/LIMITATION NOTICES: Enter any limitations on further dissemination of the report, other than those imposed by security classification, using standard statements such as:

(1) "Qualified requesters may obtain copies of this report from DDC."

(2) "Foreign announcement and dissemination of this report by DDC is not authorized."

(3) "U. S. Government agencies may obtain copies of this report directly from DDC. Other qualified DDC users shall request through _____."

(4) "U. S. military agencies may obtain copies of this report directly from DDC. Other qualified users shall request through _____."

(5) "All distribution of this report is controlled. Qualified DDC users shall request through _____."

If the report has been furnished to the Office of Technical Services, Department of Commerce, for sale to the public, indicate this fact and enter the price, if known.

11. SUPPLEMENTARY NOTES: Use for additional explanatory notes.

12. SPONSORING MILITARY ACTIVITY: Enter the name of the departmental project office or laboratory sponsoring *(paying for)* the research and development. Include address.

13. ABSTRACT: Enter an abstract giving a brief and factual summary of the document indicative of the report, even though it may also appear elsewhere in the body of the technical report. If additional space is required, a continuation sheet shall be attached.

It is highly desirable that the abstract of classified reports be unclassified. Each paragraph of the abstract shall end with an indication of the military security classification of the information in the paragraph, represented as *(TS), (S), (C), or (U).*

There is no limitation on the length of the abstract. However, the suggested length is from 150 to 225 words.

14. KEY WORDS: Key words are technically meaningful terms or short phrases that characterize a report and may be used as index entries for cataloging the report. Key words must be selected so that no security classification is required. Identifiers, such as equipment model designation, trade name, military project code name, geographic location, may be used as key words but will be followed by an indication of technical context. The assignment of links, rules, and weights is optional.

Unclassified

Security Classification

6956-66